21

Propagation Aspects in Vehicular Networks

Lorenzo Rubio[1], Juan Reig[1] and Herman Fernández[2]
[1]*Universidad Politécnica de Valencia*
[2]*Universidad Pedagógica y Tecnológica of Colombia*
[1]*Spain*
[2]*Colombia*

1. Introduction

Traffic accidents have become an important health and social problem due to the enormous number of fatalities and injuries. The total number of deaths and injuries in the European Union (EU), United States of America (USA) and Japan has been steadily reduced over the last decade. This reduction is mainly attributed to the implementation of a set of road safety measures, such as seat-belt use, vehicle crash protection, traffic-calming interventions and traffic law enforcement. However, the number of accidents has remained uniform due to the increasing number of vehicles and total distance driven (Peden et al., 2004).

In addition to passive vehicle safety systems, such as airbags, anti-lock braking system (ABS) and electronic stability control (ESP), new active safety systems have been introduced to improve vehicular safety. To this end, the last decade has witnessed the traffic management industry, engage and promote the integration of information and communications technology (wireless, computing and advanced sensor technologies) into both vehicles and the wider transport infrastructure. These proposals have led to the intelligent transportation system (ITS) concept. At present, different ITS applications have been introduced, such as variable message signs (VMS), located at strategic points (e.g., tunnels and merging highways) or spaced at given distances, to inform drivers about traffic and dangerous situations; automated toll collection systems for highways and parkings; and real-time traffic information broadcasted in the FM radio band.

Besides this, onboard ITS applications have improved the assistance and protection mechanisms for drivers: navigation systems, rear and front parking radars, and cameras are extensively used in the vehicle. Vehicles now incorporate sophisticated computing systems, with several sensors interconnected. However, short-range sensors employed in emergency systems, such as forward collision warning and lane keeping assist, are insufficient, specially when these sensors need to extend their communication horizon in emergency cases due to the limitation of their operating range to line-of-sight (LOS) conditions (Vlacic et al., 2001).

Therefore, there are safety applications for distance emergency situations, such as blind corners and traffic crossing, where large-range vehicular communication systems are required, e.g., operating rages of about 1000 meters, in both LOS and non-LOS (NLOS) conditions (Gallagher & Akatsuka, 2006). Wireless communications systems which can operate with these constraints are known as cooperative systems on the road. In the cooperative system concept, vehicles and infrastructure exchange safety messages to extend the distance horizon and provide more information in real time to drivers. Cooperative systems involve two

capabilities: vehicle-to-infrastructure (V2I) and vehicle-to-vehicle (V2V) communications. V2I and V2V communications are also referred to in the literature as V2V communications.
Government radio management organizations have been allocated specific bands for ITS throughout the world. In USA, the Federal Communication Commission (FCC) assigned 75 MHz of licensed spectrum, from 5.85 GHz to 5.925 GHz, as part of ITS for dedicated short-range communications (DSRC) in 1999. The European Telecommunication Standard Institute (ETSI) allocated 70 MHz for ITS in the 5.9 GHz band, within the frequency range from 5.850 GHz to 5.925 GHz, in 2003. This band was divided in three subbands: (1) a band of 2x10 MHz, which is prioritized for critical road safety applications, (2) 30 MHz of spectrum for road safety related applications, and (3) 20 MHz of spectrum for non-safety related applications (ETSI TR 102 492-1 Part 1, 2006), (ETSI TR 102 492-2 Part 2, 2006). In Japan, a 10 MHz band from 715 MHz to 725 MHz was assigned for ITS using V2V communications in 2007 (Sai et al., 2009). Other unlicensed bands as the 2.4 GHz or 5.4 GHz bands can be also used for non-safety ITS applications.
The protocol stack standardized for DSRC systems is known as wireless access in vehicular environments (WAVE), whose physical layer (PHY) is the IEEE 802.11p (IEEE 802.11p, 2010) which is an adaptation of the IEEE 802.11a standard (IEEE 802.11, 2007) for DSRC systems.
In order to optimize the design and development of ITS applications based on wireless systems, it is necessary to understand the propagation channel characteristics and how these can affect the final performance of safety applications, where a low latency in the communication is vital. The V2V channel, where both the transmitter and receiver can be in motion with low elevation antennas, is a relatively novel research area in channel modeling. Differences between V2V channels and fixed-to-mobile (F2M) channels make that channel models developed for F2M cannot be applied to the performance evaluation and deployment of future ITS applications based on vehicular communications systems. In addition, V2I communications in open areas, such as intercity roads, where the fixed transmitting antennas are located along the roads at low height, have not yet been sufficiently analyzed in traditional wireless communication models. Also, particular characteristics of vehicular environments, such as traffic density and vehicle speeds, have a direct influence on the final performance of vehicular safety systems. Therefore, the main features of V2X channels must be taken into account in the channel modeling and its corresponding channel model.
In the context of V2X communications under the ITS concept and vehicular safety applications, this Chapter provides an overview of propagation aspects in vehicular networks based on the available literature, inspecting the approaches introduced in vehicular channel modeling, as well as the most important channel measurement campaigns carried out to validate and develop new and more accurate channel models. Narrowband and wideband characteristics of the vehicular propagation channel are also examined. The most important path loss models published in the literature, as well as Doppler spread models and fading statistics based on channel measured data are revised. Finally, general aspects related to the antennas for vehicular communications and future advances in channel modeling are also dealt with.

2. DSRC link specifications

In 2003, the DSRC specifications for ITS applications in the 5.9 GHz band were standardized in (ASTM E2213, 2003), where the spectrum allocated in USA was divided into seven

channels of 10 MHz. The channel numbering and the maximum equivalent isotropically radiated power (EIRP) for DSRC devices are illustrated in Table 1. Channel 178 is the control channel (CCH), and it is used principally to broadcast communications related to safety applications, while non-safety data exchange is strictly limited in terms of transmission time and interval. The remaining six channels are referred to as service channels (SCH) and are dedicated to safety and non-safety applications. Channel 172 is used in V2V communications, and channel 184 is dedicated to V2I communications, especially in intersection applications. The rest of the service channels, i.e., 174, 176, 180 and 182, which may be combined in 2 channels of 20 MHz (channels 175 and 181), are used to share safety-related applications. A guard band of 5 MHz is located at the lower edge. In the EU, 20 MHz were allocated in the spectrum in the unlicensed band, from 5.795 to 5.815 GHz for short-range applications, such as electronic fee collection and parking band (ETSI EN 300 674, 1999).

Channel Number	Central frequency (MHz)	Bandwidth (MHz)	RSU EIRP max. (dBm) Pub./Priv	OBU EIRP max. (dBm) Pub./Priv
172	5860	10	33/33	33/33
174	5870	10	33/33	33/33
175	5875	20	23/33	23/33
176	5880	10	33/33	33/33
178	5890	10	44.8/33	44.8/33
180	5900	10	23/23	23/23
181	5905	20	23/23	23/23
182	5910	10	23/23	23/23
184	5920	10	40/33	40/33

Table 1. DSRC channel allocation in the 5.9 GHz ITS band

The maximum EIRP depends on the type of device. The radio transmitter onboard vehicles is called an on-board unit (OBU). The roadside unites (RSUs) are equipped within the infrastructure along the roadside. The EIRP is also limited depending on the application be it public or private. In the EU, the maximum EIRP in the ITS band was limited to 33 dBm (TR 102 492-1 Part 1, 2005). In the 5.8 GHz band, the EIRP of RSUs was also limited to 33 dBm and the maximum single side band EIRP was fixed on -21 dBm with backscattering using a passive OBU or tag (ETSI EN 300 674, 1999).

The radio specifications of ASTM E2213-03 standard are compiled in the IEEE 802.11p standard (IEEE 802.11p, 2010), which is an adaptation to vehicular radio communications of the IEEE 802.11a standard in the 5.9 GHz band (IEEE 802.11, 2007). Each channel of 10 MHz or 20 MHz is OFDM modulated using 52 subcarriers, with 4 pilots and the remaining 48 subcarriers being used for data transmission.

The main characteristics of the radio link are summarized in the Table 2. The media access control (MAC) protocol is the carrier sense multiple access with collision avoidance (CSMA/CA). Consequently, the channel is shared amongst the communication transmissions which simultaneously use this channel. The efficiency of the data rate, due to the MAC protocol, depends on the transmitter number of nodes, the transmission mode and the packet size (CEPT Report 20, 2007). Using a data rate of 6 Mbps and 100 nodes simultaneously transmitting, the efficiency varies from about 0.4 to 0.5 with a packet size of

256 and 1024 bytes, respectively, which correspond to a shared data rate of 2.4 Mbps and 3 Mbps, respectively.

Channel bandwidth	10 MHz	20 MHz
RF link range (m)	1000[1]	
Average LOS packet error rate (%)	10	
Average NLOS packet error rate (%)	Not defined	
Transmitted output power class (dBm)	0, 10, 20, 29 (Class A, B, C, D)	
Modulations	BPSK[2], QPSK[3], 16 QAM, 64 QAM	
Channel data rates (Mbps)	3, 4.5, 6[3], 9, 12, 18, 24, 27	6, 9, 12, 18, 24, 36, 48, 54
Receiver sensitivities (dBm)	-85 (3 Mbps), -84 (4.5 Mbps), -82 (6 Mbps), -80 (9 Mbps), -77 (12 Mbps), -73 (18 Mbps), -69 (24 Mbps), -68 (27 Mbps)	-82 (6 Mbps), -81 (9 Mbps), -79 (12 Mbps), -77 (18 Mbps), -74 (24 Mbps), -70 (36 Mbps), -66 (48 Mbps), -65 (54 Mbps)
Number of receiver antennas	1 (default)	
Maximum speed vehicle	200 km/h (120 mph)	
Packet size (bytes)	64, 1000[4]	
Maximum latency	From 20 ms to 1 s[5]	
OFDM symbol duration (μs)	8	4

Table 2. DSRC physical specifications (ASTM E2213-03, 2003), (IEEE 802.11p, 2010)

From channel measurements carried out in a highway environment under real traffic conditions, LOS ranges varying from 880 m to 1327 m in V2V and V2I links were achieved, respectively (Gallagher & Akatsuka, 2006). The measured packet error rate oscillates from 0.63% (V2V) to 1.21% (V2I). A coverage distance from 58 m to 230 m was obtained under NLOS conditions for V2V radio links.

3. Vehicular channel modeling

In any wireless communication, there are numerous interacting objects (reflectors and/or scatterers) between the transmitter and the receiver which condition the radio propagation, such as mountains, buildings, trees, vehicles, etc. that comprise the propagation environment. In the receiving antenna, multiple contributions or replicas of the transmitted signal will be received. These replicas will suffer different reflection, diffraction and scattering processes. The received signal corresponds to the coherent addition of these

[1] This range corresponds to the ASTM E2213-03 specification. The required range depends on the application. The range oscillates from 50 m in precrash sensing to 1000 m for approaching emergency vehicle warning or emergency vehicle signal preemption services (Almalag, 2009).
[2] The first OFDM symbol is always BPSK modulated.
[3] The control channel uses 10 MHz of bandwidth, with QPSK modulation and 6 Mbps data rate.
[4] These packet sizes correspond to ASTM E2213-03. However, the packet size depends on the application characteristics. The message length oscillates from 150 bytes to 1200 bytes (CEPT Report 20, 2007).
[5] The maximum allowed latency depends on the application. The maximum latency oscillates from 20 ms in precrash sensing and 1 s in various sign extension applications (Almalag, 2009).

replicas, in amplitude and phase. Such replicas have different attenuation and delay related to the travelled propagation path. Then, the received signal can experience time-dispersion (frequency-selectivity) due to the multipath propagation. In addition, due to the motion of the terminals, or the movement of any interacting object in the propagation environment, the received signal can experience time-selectivity (frequency-dispersion), as a consequence of changes in the phase relationship among the received replicas. In these conditions, the propagation environment will limit the final quality of any wireless communication system, obliging to the implementation of different transmission techniques to mitigate the impairments caused by the channel, such as diversity, equalization, power control and error correction, among others.

The term *channel modeling*, also referred to as *channel characterization*, is used to describe the approaches, models, and channel measurements conducted to understand how the propagation channel impairs and distorts the transmitted signal that propagates through it in a specific environment. The different propagation processes that can occur in wireless channels, i.e., free-space, diffraction, reflection, scattering and transmission through irregular objects, make difficult channel modeling. For practical purposes, it is necessary to adopt some approaches and simplifications of the propagation environment. Therefore, a *channel model* is a simplified representation of the propagation channel centered on those aspects of the propagation channel that can significantly affect the final performance of the wireless system (Michelson & Ghassemzadeh, 2009). In this sense, a channel model can be considered as a set of parameters which describes the propagation paths characteristics allowing one to analyze, simulate and design wireless communication systems. The knowledge of the propagation phenomenon and an accurate channel model are essential for a flexible and practical design of any wireless communications system under realistic propagation conditions.

Wireless channel investigation has decades of history encompassing the deployment of mobile and personal communication systems (cellular systems) in the early eighties. Nevertheless, the vehicular channel, in which both the transmitter and receiver can be in motion, is at present an important area in channel modeling (Matolak and Wu, 2009), (Wang et al., 2009) and (Molisch et al., 2009). The interest in vehicular channel modeling is mainly motivated by the ITS concept for dedicated short-range communications in vehicular environments, together with the appearance of new applications related to driving safety, that makes the knowledge of the V2V and V2I channels of paramount importance for the design and performance evaluation of vehicular communication systems.

The motion of terminals and the use of low elevation antennas make V2V systems differ from conventional F2M or cellular systems, where the base station is fixed with a height greater than the mobile terminal. Another difference with cellular systems is the high mobility that can be observed in V2V systems due to the relative velocities of the vehicular terminals. The high mobility makes vehicular channels exhibit greater temporal variability than other conventional channels, such as F2M channels, and can suffer more severe fast fading. On the other hand, the probability of link obstruction increases as a consequence of both the interacting objects displacement and the use of low elevation antennas. These differences, together with different frequency bands operation, make that the channel knowledge and channel models developed for cellular systems cannot be used in the performance evaluation and deployment of future V2V communication systems.

The high dynamics experienced in vehicular environments and multipath propagation cause vehicular channels to be both time- and frequency-selective. The time-selectivity refers

to channel changes over time due to the motion of both terminals and scatterers. In the frequency domain, time-selectivity appears as frequency-dispersion. The frequency-selectivity refers to the variations of the channel in the frequency. In the time domain, frequency-selectivity reverts to time-dispersion.

The channel parameters describing the time- and frequency-dispersion are closely related to the environment where the propagation occurs. From a channel modeling point of view, the main features of the vehicular environment which are necessary to take into account are the following: (1) type of propagation link (V2V or V2I), (2) type of environment (urban, suburban, rural, expressway, highway, open areas, etc.), (3) vehicles speeds, (4) vehicular traffic density, and (5) direction of motion of the transmitter and receiver vehicles (the same or in opposite directions). Although some of the above features are overlapped, for example traffic densities are usually higher in urban environments and higher vehicle speeds are given in expressway and highway environments, these features increase the possible combinations of real propagation conditions thus making difficult the development of deterministic propagation models. Therefore, the characteristics of vehicular propagation channels are mainly determined either by means of (1) simulation models or (2) through measurement campaigns collected using a channel sounder in the time or frequency domain. Also, from a system design point of view, due to the large possible combinations of real propagation conditions, transmission techniques incorporated to reduce channel impairments will observe channels with different time (delay) and frequency (Doppler) dispersion.

Next, Subsection 3.1 is oriented towards the introduction of the most common parameters used in channel modeling to describe the time- and frequency-dispersive behavior, in a general wireless channel. A review of the most important V2V channel models and the approaches made to build them is presented in the Subsection 3.2.

3.1 Parameters for characterizing wireless channels

The most important parameters used to describe wireless channels, in a deterministic or statistical sense, can be derived from the channel impulse response (CIR). We will introduce the CIR of a time-variant wireless channel, as the basis to make a description of the time- and frequency-dispersive behavior of the channel.

In a time-variant environment characterized by multipath propagation, the received signal can be seen as the temporal superposition of the transmitted signal replicas (contributions from reflectors and scatterers) with different attenuation and delay. If the transmitted bandpass signal, denoted by $s(t)$, is

$$s(t) = \mathrm{Re}\left\{ s_p(t) \exp\left(j2\pi f_c t \right) \right\}, \tag{1}$$

where $s_p(t)$ is the complex envelope and f_c being the carrier frequency, the bandpass received signal, denoted by $y(t)$, is given by

$$\begin{aligned} y(t) &= \mathrm{Re}\left\{ \sum_{k=1}^{\infty} \sum_{i=1}^{\infty} a_{k,i} s_p\left(t - \tau_i\right) \exp\left(j2\pi \left(f_c + f_d \cos\theta_{k,i} \right) t + \phi_{k,i} \right) \right\} \\ &= \mathrm{Re}\left\{ \left[\sum_{i=1}^{\infty} h(t, \tau_i) \delta\left(t - \tau_i\right) \otimes s_p(t) \right] \exp\left(j2\pi f_c t \right) \right\} = \mathrm{Re}\left\{ \left[h(t,\tau) \otimes s_p(t) \right] \exp\left(j2\pi f_c t \right) \right\} \end{aligned} \tag{2}$$

where

$$h(t,\tau_i) = \sum_{k=0}^{\infty} a_{k,i} \exp\left(j2\pi f_d \cos\theta_{k,i} t + \phi_{k,i}\right), \tag{3}$$

and

$$h(t,\tau) = \sum_{i=0}^{\infty} h(t,\tau_i)\delta(\tau - \tau_i), \tag{4}$$

with $a_{k,i}$ and $\phi_{k,i}$ being the amplitude and phase of the *i*-th contribution that arrives to the receiver with an angle $\theta_{k,i}$ with respect to the direction of motion, and delay τ_i. The term f_d is the maximum Doppler frequency, also called Doppler shift, i.e., $f_d = v / \lambda_c$, where v refers to the receiver velocity, $\lambda_c = c_0 / f_c$ is the wavelength associated to the carrier frequency f_c, and c_0 is the speed of light. The $\delta(\cdot)$ function is the Dirac delta, and $\otimes$ denotes convolution. Eq. (4) corresponds to the time-variant impulse response of the wireless radio channel. Specifically, $h(t,\tau)$ is the response of the lowpass equivalent channel at time t to a unit impulse generated τ seconds in the pass (Parsons, 2000). $h(t,\tau)$ is known as the *input delay-spread function*, and is one of the four system functions described by Bello (Bello, 1963), which can be used to fully characterize linear time-variant (LTV) radio channels. The term $h(t,\tau_i)$ is the time-dependent complex coefficient associated to a delay τ_i, and can be expressed as

$$h(t,\tau_i) = h_{iR}(t) + jh_{iQ}(t), \tag{5}$$

where

$$h_{iR}(t) = \sum_{k=0}^{\infty} a_{k,i} \cos\left(2\pi f_d \cos\theta_{k,i} t + \phi_{k,i}\right) \tag{6}$$

and

$$h_{iQ}(t) = \sum_{k=0}^{\infty} a_{k,i} \sin\left(2\pi f_d \cos\theta_{k,i} t + \phi_{k,i}\right) \tag{7}$$

are the in-phase and quadrature components, respectively.

In practice, many physical channels can be considered stationary over short periods of time, or equivalently over small spatial distances due to the transmitter/receiver or interacting objects displacement. Although these channels may not be necessarily stationary in a strict sense, they usually are considered wide sense stationary (WSS) channels. Also, a channel can exhibit uncorrelated scattering (US) in the time variable, i.e., contributions with different delays are uncorrelated. The combination of the WSS and US assumptions yields the WSSUS assumption, which has been very used in channel modeling for cellular systems.

Under the WSSUS assumption, the channel can be represented as a tapped delay line (TDL), where the CIR is written as

$$h(t,\tau) = \sum_{i=1}^{N} h_i(t)\delta(\tau - \tau_i), \tag{8}$$

where $h_i(t) \triangleq h(t,\tau_i)$ refers to the complex amplitude of the *i*-th tap. Using this representation of the CIR, and taking into account Eq. (3), each of the *N* taps corresponds to one group of closely delayed/spaced multipath components (MPCs). This representation is commonly used in the channel characterization theory because the time resolution of the receiver is not sufficient to resolve all MPCs in most practical cases. It is worth noting that the number of taps, *N*, and MPCs delay associated to the *i*-th tap, τ_i, remain constant during a short period of time, where the WSS assumption is valid. For this reason, *N* and τ_i are not dependent on the time variable in Eq. (8). Fig. (1) shows a graphical representation of the TDL channel model based on delay elements.

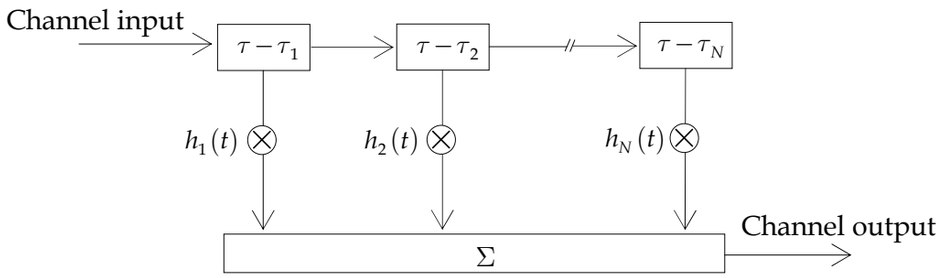

Fig. 1. TDL channel model description based on delay elements

The time variation of the taps complex amplitude is due to the MPCs relative phases that change in time for short displacements, in terms of the wavelength, of the transmitter/receiver and/or interacting objects. Thereby, $h_i(t)$ is referred to in the literature as the *fading complex envelope* of the *i*-th path. The time variation of $h_i(t)$ is model through the Rayleigh, Rice or Nakagami-*m* distributions, among others (for a mathematical description of these distributions, the reader is referred to the Section 5 of this Chapter).
As introduced previously, vehicular environments can be dynamic due to the movement of the terminals and/or the interacting objects. Therefore, vehicular channels may be non-stationary and the channel statistics and the CIR can change within a rather short period of time. In this situation, the WSSUS assumption is not applicable anymore. Sen and Matolak proposed to model the non-stationarities of vehicular channels through a *birth/death persistence process* in order to take into account the appearance and disappearance of taps in the CIR (Sen & Matolak, 2008). Then, the CIR can be rewritten as

$$h(t,\tau) = \sum_{i=1}^{N} h_i(t) z_i(t) \delta(\tau - \tau_i), \tag{9}$$

where $z_i(t)$ is introduced to model the birth/death persistence process. $z_i(t)$ takes the 0 and 1 values to model the disappearance and appearance of the *i*-th tap, respectively. As appointed in (Molish et al., 2009), this persistence process can provide a non-stationarity of the channel, but it does not consider the drift of scatterers into a different delay bin, and as result can lead to the appearance or disappearance of sudden MPCs. The non-stationarity

problem in V2V channel has been also addressed in (Bernardó et al., 2008) and (Renaudin et al., 2010) from channel measurement data.
The dispersive behavior in the time and frequency domains of any wireless channel conditions the transmission techniques designed to mitigate the channel impairments and limits the system performance. As an example, time-dispersion (or frequency-selectivity) obliges to implement equalization techniques, and frequency dispersion (or time selectivity) forces the use of diversity and adaptive equalization techniques. Orthogonal frequency division multiplexing (OFDM) has been suggested to be used in IEEE 802.11p. In a V2V system based on OFDM, time-dispersion fixes the minimum length of the cyclic prefix, and frequency-dispersion can lead to inter-carrier interference (ICI). In the following, the most important parameters used to describe the time- and frequency-dispersion behavior will be introduced.

3.1.1 Time-dispersion parameters

For a time-varying channel with multipath propagation, a description of its time-dispersion characteristics can be obtained by expressing the autocorrelation function of the channel output (the received signal) in terms of the autocorrelation function of the *input delay-spread function*, denoted by $R_h(t,s;\tau,\eta)$ and defined as

$$R_h(t,s;\tau,\eta) \triangleq E\left\{h(t,\tau)h^*(s,\eta)\right\}, \tag{10}$$

where $E\{\cdot\}$ is the expectation operator. In Eq. (10) t and s are time variables, whereas τ and η correspond to delay variables. If the WSSUS assumption is considered, the autocorrelation function of the channel output can be described by the *delay cross-power spectral density*, denoted by $P_h(\xi,\tau)$, where $\xi = s - t$ is a short time interval in which the channel can be considered wide-sense stationary. The WSSUS assumption implies a small-scale characterization of the channel where a local scattering can be observed, i.e., short periods of time or equivalently short displacements of the terminals. When $\xi \to 0$, $P_h(\xi,\tau)$ is simplified by $P_h(\tau)$, which is referred to as *power delay profile* (PDP) in the literature
It is very common in the wideband channel characterization theory to express the time- and frequency-dispersion of a wireless channel by means of the *delay-Doppler cross-power spectral density*, also called *scattering function*[6], denoted by $P_S(\tau,\nu)$, where the ν variable refers to the Doppler shift. The scattering function can be regarded as the Fourier transform of the autocorrelation function $R_h(t,t+\xi;\tau,\eta) \equiv R_h(\xi;\tau,\eta) = \delta(\eta-\tau)P_h(\xi,\tau)$ with respect to the ξ variable. For a complete understanding of a stochastic wideband channel characterization, the reader can see the Reference (Parsons, 2000), widely cited in channel modeling studies.
From $P_S(\tau,\nu)$, $P_h(\tau)$ can be also derived integrating the scattering function over the Doppler shift variable, i.e.

$$P_h(\tau) = \int_{-\infty}^{+\infty} P_S(\tau,\nu)\,d\nu\,. \tag{11}$$

[6] The term scattering function was incorporated in the wireless channels characterization due to the $P_S(\tau,\nu)$ function is identical to the scattering function $\sigma(\tau,\nu)$ of a radar target.

From channel measurements of the CIR in a particular environment, and assuming ergodicity, the $P_h(\tau)$ can also be estimated for practical purposes as

$$P_h(\tau) = E_t\left\{\left|h(t,\tau)\right|^2\right\}, \tag{12}$$

where $E_t\{\cdot\}$ denotes expectation in the time variable. From Eq. (12), the PDP can be seen as the squared magnitude of the CIR, averaged over short periods of time or small local areas around the receiver (small-scale effect).

The most important parameter to characterize the time-dispersion behavior of the channel is the *rms* (root mean square) delay spread, denoted by τ_{rms}, which corresponds to the second central moment of the PDP, expressed as

$$\tau_{rms} \triangleq \sqrt{\frac{\int_0^\infty (\tau-\overline{\tau})^2 P_h(\tau)\,d\tau}{\int_0^\infty P_h(\tau)\,d\tau}}, \tag{13}$$

where $\overline{\tau}$ is the average delay spread, or first central moment of the PDP, given by

$$\overline{\tau} \triangleq \frac{\int_0^\infty \tau P_h(\tau)\,d\tau}{\int_0^\infty P_h(\tau)\,d\tau}. \tag{14}$$

Other metrics to describe the delay spread of wireless channels are the maximum delay spread, the delay window and the delay interval (Parsons, 2000).

The frequency-selective behavior of wireless channels is described using the *time-frequency correlation function*, denoted by $R_T(\Omega,\xi)$ [7], which is the Fourier transform of the $P_h(\xi,\tau)$ function over the delay variable, i.e.

$$R_T(\Omega,\xi) = \int_{-\infty}^{+\infty} P_h(\xi,\tau)\exp\{-j2\pi\Omega\tau\}\,d\tau. \tag{15}$$

The Ω variable refers to a frequency interval, i.e., $\Omega = f_2 - f_1$. When $\xi = 0$, expression (15) is written as

$$R_T(\Omega) = \int_{-\infty}^{+\infty} P_h(\tau)\exp\{-j2\pi\Omega\tau\}\,d\tau, \tag{16}$$

where $R_T(\Omega)$ is known as the *frequency correlation function*. A metric to measure the frequency-selectivity of the channel is the coherence bandwidth, denoted by B_C. From Eq. (16), B_C is the smallest value of Ω for which the normalized frequency correlation function, denoted by $\tilde{R}_T(\Omega) \triangleq R_T(\Omega)/\max\{R_T(\Omega)\}$, where $\max\{R_T(\Omega)\} = R_T(\Omega=0)$, is equal to some suitable correlation coefficient, e.g. 0.5 or 0.9 are typical values. Physically, the coherence bandwidth represents the channel bandwidth in which the channel experiences approximately a flat frequency response behavior.

[7] $R_T(\Omega,\xi)$ corresponds to the autocorrelation function of the *time-variant transfer function* $T(f,t)$.

Since $P_h(\tau)$ is related to $R_T(\Omega)$ by the Fourier transform, there is an inverse relationship between the *rms* delay spread and the coherence bandwidth, i.e., $B_C \propto 1/\tau_{rms}$.

3.1.2 Frequency-dispersion parameters

When a channel is time-variant, the received signal suffers time-selective fading and as a result frequency-dispersion occurs. A description of the frequency-dispersion characteristics can be derived from the *Doppler cross-power spectral density*, denoted by $P_H(\Omega,\nu)$. In a WSSUS channel, $P_H(\Omega,\nu)$ is related to the autocorrelation of the *output Doppler-spread function*, denoted by $R_H(\Omega;\nu,\mu)$,

$$R_H(f, f+\Omega;\nu,\mu) = \delta(\nu-\mu)\, P_H(\Omega,\nu), \tag{17}$$

where the autocorrelation function is defined as

$$R_H(f,m;\nu,\mu) \triangleq E\left\{H(f,\nu)H^*(m,\mu)\right\}, \tag{18}$$

being $H(f,\nu)$ the *output Doppler-spread function*. In Eq. (18) f and m are frequency variables, whereas ν and μ correspond to Doppler shifts variables. From the relationships between the autocorrelation functions in a WSSUS channel (Parsons, 2000), the $P_H(\Omega,\nu)$ function can also be regarded as the Fourier transform of the scattering function with respect to the τ variable. When $\Omega \to 0$, $P_H(\Omega,\nu)$ is simplified by $P_H(\nu)$, which is referred to in the literature as *Doppler power density spectrum* (PDS). In a similar manner to the PDP, the Doppler PDS can also be derived integrating the scattering function over the delay variable, i.e.

$$P_H(\nu) = \int_{-\infty}^{+\infty} P_S(\tau,\nu)\, d\tau\,. \tag{19}$$

Now, from the Doppler PDS some parameters can be defined to describe the frequency-dispersive behavior of the channel. The most important parameter is the *rms* Doppler spread, denoted by ν_{rms}, given by

$$\nu_{rms} \triangleq \sqrt{\frac{\int_0^{\infty} (\nu-\overline{\nu})^2 P_H(\nu)\, d\nu}{\int_0^{\infty} P_H(\nu)\, d\nu}}, \tag{20}$$

where $\overline{\nu}$ is the average Doppler spread, or first central moment of the Doppler PDS, given by

$$\overline{\nu} \triangleq \frac{\int_0^{\infty} \nu P_H(\nu)\, d\nu}{\int_0^{\infty} P_H(\nu)\, d\nu}. \tag{21}$$

Time-selective fading refers to the variations of the received signal envelope due to the movement of the transmitter/receiver and/or the interacting objects in the environment. This displacement causes destructive interference of MPCs at the receiver, which arrive with different delays that change in time or space. This type of fading is observed on spatial

scales in terms of the wavelength, and is referred to in the literature as *small-scale fading* in opposite to the *large-scale fading* (also referred to as *shadowing*) due to the obstruction or blockage effect of propagation paths. The variation of the received signal envelope can also be modeled in a statistical way using the common Rayleigh, Rice or Nakagami-*m* distributions.

In a similar manner to the coherence bandwidth, for a time-variant channel it is possible to define a parameter called *coherence time*, denoted by T_C, to refer to the time interval in which the channel can be considered stationary. From the *time correlation function of the channel*, denoted by $R_T(\xi) \equiv R_T(\Omega \to 0, \xi)$, T_C is the smallest value of ξ for which the normalized time correlation function, denoted by $\tilde{R}_T(\xi) \triangleq R_T(\xi) / \max\{R_T(\xi)\}$, where $\max\{R_T(\xi)\} = R_T(\xi = 0)$, is equal to some suitable correlation coefficient, e.g., 0.5 and 0.9 are typical values. There is an inverse relationship between the *rms* Doppler spread and the coherence time, i.e., $T_C \propto 1 / \nu_{rms}$.

3.2 V2V channel models

In the available literature of channel modeling, one can find different classifications of wireless channel models, e.g., narrowband or wideband models, non-physical (analytical) and physical (realistic) models, and two-dimensional or three-dimensional models, among others. Regardless of the type of classification, wireless channel models are mainly based on any of the three following approaches (Molish & Tufvesson, 2004):

- *deterministic* approach, which characterizes the physical propagation channel using a geographical description of the environment and *ray approximation*[8] techniques (ray-tracing/launching),
- *stochastic* approach, oriented to the channel parameters characterization in terms of probability density functions often based on large measurement campaigns, and
- *geometry-based stochastic* (GBS) approach, which assumes a stochastic distribution of interacting objects around the transmitter and the receiver and then performing a deterministic analysis.

In the following, some published V2V channels models based on these approaches will be briefly introduced. Also, the main advantages and drawbacks when the above approaches are applied to V2V channel models will be indicated.

3.2.1 Deterministic models

A deterministic channel model[9] characterizes the physical channel parameters in specific environments solving the Maxwell's equations in a deterministic way, or using analytical descriptions of basic propagation mechanisms (e.g., free-space propagation, diffraction, reflection and scattering process). These models require a geographical description of the environment where the propagation occurs, together with the electromagnetic properties of the interacting objects. It is worth noting that the term *deterministic* refers to the way in which the propagation mechanisms are described. Evidently, the structure of interacting objects, their electrical parameters (e.g., the conductivity and permittivity), and some parts

[8] Ray approximation techniques refer to high frequency approximations, where the electromagnetic waves are modeled as rays using the geometrical optic theory.

[9] Deterministic models are also referred to in the literature as geometric-based deterministic models (GBDMs).

of the environment are introduced in the model in a simple way by means of simplified or idealistic representations. The main drawbacks of deterministic models are the large computational load and the need of a geographical database with high resolution to achieve a good accuracy. Therefore, it is necessary to seek a balance between computational load and simplified representations of the environment elements. On the other hand, deterministic models have the advantage that computer simulations are easier to perform than extensive measurements campaigns, which require enormous effort.
The use of deterministic models based on ray-tracing techniques allows us to perform realistic simulations of V2V channels. Earlier Reference (Maurer et al., 2001) presents a realistic description of road traffic scenarios for V2V propagation modeling. A V2V channel model based on ray-tracing techniques is presented in (Maurer et al., 2004). The model takes into account the road traffic and the environment nearby to the road line. A good agreement between simulations results, derived from the model, and wideband measurements at 5.2 GHz was achieved. Nevertheless, characteristics of vehicular environments and the resulting large combinations of real propagation conditions, make difficult the development of V2V deterministic models with certain accuracy.

3.2.2 Stochastic models

Stochastic models[10] describe the channel parameters behavior in a stochastic way, without knowledge of the environment geometry, and are based on measured channel data.
For system simulations and design purposes, the TDL channel model has been adopted due to its low complexity. The parameters of the TDL channel model are described in a stochastic manner. Reference (Acosta-Marum & Ingram, 2007) provides six time- and frequency-selective empirical models for vehicular communications, three models for V2V and another three for V2I communications. In these models, the amplitude of taps variations are modeled in a statistical way through the Rayleigh and Rice distributions, with different types of Doppler PDS. The models have been derived from channel measurements at 5.9 GHz in different environments (expressway, urban canyon and suburban streets). In the references (Sen & Matolak, 2007), (Sen & Matolak, 2008) and (Wu et al., 2010), complete stochastic models based on the TDL concept are provided in the 5 GHz frequency band for several V2V settings: urban with antennas inside/outside the cars, small cities and open areas (highways) with either high or low traffic densities. These models introduce the Weibull distribution to model the amplitude of taps variations. The main drawback of V2V stochastic models based on the TDL representation is the non-stationary behavior of the vehicular channel. To overcome this problem, Sen and Matolak have proposed a birth/death (on/off) process to consider the non-stationarity persistence feature[11] of the taps, modeled using a two-state first-order Markov chain (Sen & Matolak, 2008).

3.2.3 Geometry-based stochastic models

The deterministic and stochastic approaches can be combined to enhance the efficiency of the channel model, resulting in a geometry-based stochastic model (GBSM) (Molisch, 2005). The philosophy of GBSMs is to apply a deterministic characterization assuming a stochastic (or randomly) distribution of the interacting objects around the transmitter and the receiver

[10] In the literature, stochastic models are also referred to as non-geometrical stochastic models (NGSMs)
[11] The persistence process is modeled by $z(t)$ in Eq. (9).

positions. To reduce computational load, simplified ray-tracing techniques can be incorporated, and to reduce the complexity of the model, it can be assumed that the interacting objects are distributing in regular shapes.

The earlier GBSM oriented to mobile-to-mobile (M2M) communications was proposed in (Akki & Haber, 1986). Akki and Haber extended the one-ring scattering model[12] resulting in a two-ring scattering model, i.e., one ring of scatterers around the transmitter and other ring around the receiver. Recent works (Wan & Cheng, 2005) and (Zajic & Stüber, 2008) consider the inclusion of deterministic multipath contributions (LOS or specular components) combined with single- and double-bounced scattering paths. Recently, in (Cheng et al., 2009) a combination of the two-ring and the ellipse scattering model is provided to cover a large variety of scenarios, for example those where the scattering can be considered non-isotropic. Fig.2 (a) shows a typical V2V urban environment, and its corresponding geometrical description, based on two-ring and one ellipse where the scatterers are placed, is illustrated in Fig.2 (b), intuitively. To take into account the scatterers around the transmitter or the receiver in expressway/highway with more lanes than in urban/suburban environments, several rings of scatterers can be considered around the transmitter/receiver in the geometrical description of the propagation environment, resulting in the so-called multi-ring scattering model.

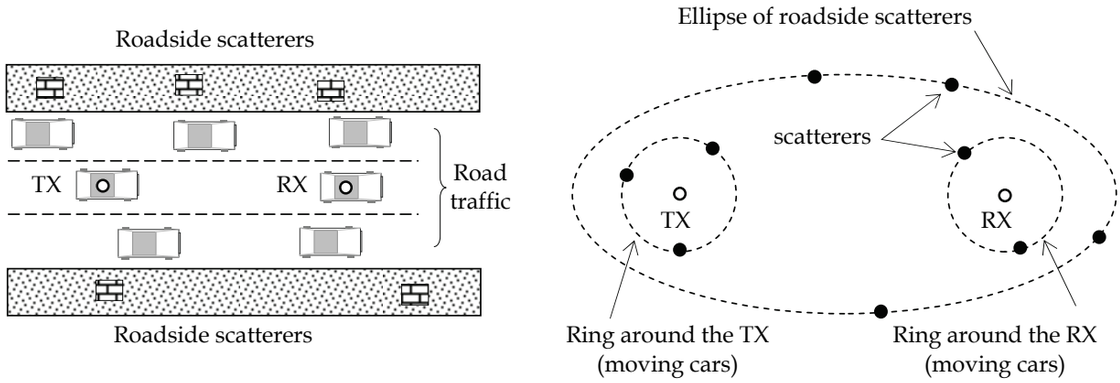

Fig. 2. Illustration of the concept of the two-ring and ellipse scattering model: (a) typical V2V urban environment with roadside scatterers along the route and road traffic (moving cars), and (b) its corresponding geometrical description to develop a GBSM

As pointed out previously, the channel parameters in vehicular environments are affected by traffic conditions. The effect of the vehicular traffic density (VTD) can be also incorporated in GBSMs. In the Reference (Cheng et al., 2009), a model that takes into account the impact of VTD on channel characteristics is presented. In Section 3.1, the problem of non-stionarity in vehicular environments due to high mobility of both the terminals and interacting objects was introduced. One advantage of GBSMs is that non-stationarities can

[12] The origin of the GBSMs goes back to the 1970s, with the introduction of antenna diversity techniques at the Base Stations in cellular systems. To evaluate the performance of diversity techniques, a set of scatterers distributed in a ring around the mobile terminal was considered.

be handled. In a very dynamic channel, as is the case of the V2V channel under high speeds and VTDs conditions, the WSSUS assumption cannot be accomplished. Results presented in (Karedal et al., 2009) show as MPCs can move through many delay bins during the terminal movement.

The manner in which GBSMs are built, permits a complete wideband channel description, as well as to derive closed-form expressions of the channel correlation functions. The latter is especially interesting in MIMO (Multiple-Input Multiple-Output) channel modeling, where the space-time correlation function[13] can be derived. The potential spectral efficiency increment of the system when MIMO techniques are introduced, together with the capability of placing multielement antennas in vehicles with large surfaces, makes MIMO techniques very attractive for V2V communications systems. The advantage of MIMO techniques, together with the MIMO channel modeling experience, explains that most of the emerging V2V GBSMs are oriented to MIMO communications. It is worth noting that MIMO techniques have generated a lot of interest and are an important part of modern wireless communications, as in the case of IEEE 802.11 standards.

The grade of accuracy in a GBSM can be increased introducing certain information or channel parameters derived from real channel data (e.g., path loss exponent and decay trend of the PDP). Reference (Karedal et al., 2009) provides a MIMO GBSM based on the results derived from an extensive MIMO measurements campaign carried out in highway and rural environments at 5.2 GHz. The model described in this reference introduces a generalization of the generic GBS approach for parameterizing it from measurements. Karedal et al. categorize the interacting objects in three types: mobile discrete scatterers (vehicles around the transmitter and receiver), static discrete scatterers (houses and road signs on and next to the road), and diffuse scatterers (smaller objects situated along the roadside).

Another important aspect to take into account in channel modeling is the three-dimensional (3D) propagation characteristics when geographical data are available. In channel modeling is frequent to distinguish between vertical and horizontal propagation. Vertical propagation takes into account the propagation mechanisms that take place in the vertical (elevation) plane, whereas horizontal propagation considers the propagation mechanisms that appear in the horizontal (azimuth) plane. The first models developed for cellular systems considered the propagation mechanisms in the vertical plane (e.g., Walfisch-Bertoni path loss model), resulting in the so-called two-dimensional (2D) models. These models were oriented to the narrowband channel characterization describing the path loss. Afterwards, the introduction of propagation mechanisms in the horizontal plane made possible a wideband characterization, resulting in 3D models. Although the V2V models cited in this section permit a wideband characterization, they only consider propagation mechanism in the horizontal plane. The assumption of horizontal propagation can be accomplished for vehicular communications in rural areas (Zajic & Stüber, 2009), whereas it can be questionable in urban environments, in which the height of the transmitting and the receiving antennas is lower than the surrounding buildings, or where the urban orography determines that the transmitter is at a different height than the receiver. For non-directional antennas in the vertical plane, the scattered/diffracted waves from the tops of buildings to the receiver located on the street are not necessarily in the horizontal plane. In this situation, a 3D propagation characterization can improve the accuracy of the channel model. The

[13] The space-time correlation function in MIMO theory can be use to compare the outage capacity of different arrays antenna geometries (i.e., linear, circular or spherical antenna array).

viability of 3D V2V GBSMs based on the two-cylinder model, as an extension of the one-cylinder model proposed by Aulin for F2M systems (Aulin, 1979), has been verified by Zajic et al. from channel measurements in urban and expressway environments (Zajic et al., 2009). The two-cylinder model can also be extended to a multi-cylinder in a similar way to the multi-ring scattering model.

4. Vehicular channel measurements

Channel measurements are essential to understand the propagation phenomenon in particular environments, and can be used to validate and improve the accuracy of existing channel models. A channel model can also take advantage of measured channel data, e.g., parameters estimated from channel measurements can be included in the channel model.

4.1 Channel measurement techniques and setups

The measurement setup used to measure the transfer function of a wireless channel, in either the time or frequency domain, is referred to as a *channel sounder*. The configuration and implementation of a channel sounder are related to the channel parameters to be measure. Thus, channel sounders may be classified as narrowband and wideband.

Narrowband channel sounders are used to make a narrowband channel characterization. Generally, the narrowband channel parameters explored are path loss, Doppler effect and fading statistics (small- and large-scale fading). The simplest narrowband channel sounder consists of a single carrier transmitter (RF transmitter) and a narrowband receiver (e.g., a specific narrowband power meter or a spectrum analyzer) to measure the received signal strength. Also, it is possible to use a vector signal analyzer (VSA) as a receiver. Since the channel response is measured at a single frequency, the time resolution of a narrowband channel sounder is infinity. This means that it is not possible to distinguish different replicas of the transmitted signal in the time delay domain.

When a wireless system experiences frequency-selectivity, or time-dispersion, a wideband characterization is necessary to understand the channel frequency-selective behavior. This is the case of the future DSRC system, which will use a minimum channel bandwidth of 10 MHz. To estimate the time-dispersion metrics defined in Section 3.1, a wideband channel sounder must be used. Wideband channel sounders can measure the channel response in either the frequency or time domain. In the frequency domain, a wideband channel sounder measures the channel frequency response at the t_0 instant, denoted by $T(f,t_0)$[14], and the CIR is estimated applying the inverse Fourier transform with respect to the frequency f variable, yielding $h(t_0,\tau)$. A vector network analyzer (VNA) can be use to estimate the channel frequency response from the S_{21} scattering parameter, where the DUT (dispositive under test) is the propagation channel and the transmitting and receiving antennas[15]. The main drawbacks of using a VNA are that the channel must be stationary during the acquisition time of the frequency response, i.e., the acquisition time must be lower than the

[14] $T(f,t)$ is the time variant transfer function of the propagation channel.

[15] When a VNA is used, the frequency response measured takes into account the channel responses and the frequency response of the transmitting and receiving antennas. A calibration process is necessary to extract the antennas effect.

coherence time of the channel, and the short transmitter-receiver separation distances since the transmitting and receiving antennas must be connected to the VNA. Due to these drawbacks, a VNA cannot be used in vehicular channel measurements. The VNA has been frequently used as a wideband channel sounder to measure the CIR over short distances, e.g., indoor scenarios. An alternative approach consists of transmitting a multicarrier signal, with known amplitudes and relative phases. As a receiver, a VSA can be used to estimate the measured complex frequency spectrum.

In the time domain, the CIR is measured directly. There are two possible implementations of wideband channel sounders operating in the time domain. The first implementation consists of using an impulse generator at the transmitter and a digital sampling oscilloscope (DSO) at the receiver, resulting in the so-called *impulse channel sounder*. The main drawback of an impulse channel sounder is that a probe antenna for the trigger pulse is necessary. Impulse channel sounders have been used in ultra-wideband (UWB) channel measurements. The second implementation of a wideband channel sounder in the time domain is based on the transmission of a wideband pseudo-random noise (PN) sequence[16]. The CIR is estimated as the cross-correlation between the received signal and the transmitted PN sequence, resulting in the so-called *correlative channel sounder*. Fig. 3 shows the operating principle of a correlative channel sounder. The correlative channel sounder is commonly used in wideband channel measurements, particularly in vehicular channel measurements. The time resolution of a correlative channel sounder and the maximum resolvable delay are related to the chip duration and the length of the PN sequence, respectively. In practice, the simplest correlative channel sounder consists of an arbitrary waveform generator (WG) as transmitter and a VSA as receiver. The WG transmits a PN sequence, the VSA collects the in-phase and quadrature components of the received signal, and then through post-processing the CIR is estimated.

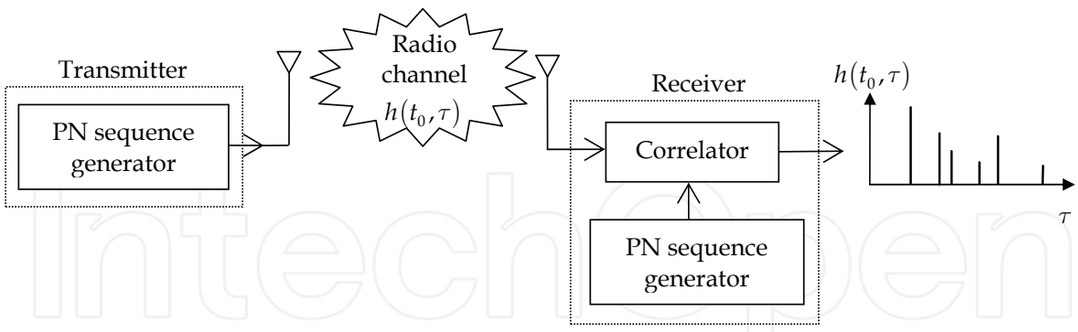

Fig. 3. Correlative channel sounder based on the PN signal principle

A wideband channel sounder can also use multiple antennas (array antennas) at the transmitter and the receiver to explore aspects related to the directional character of the propagation channel, e.g. correlation degree among the received signal at each antenna element used in spatial diversity and MIMO techniques. In MIMO channel modeling, a full characterization of the channel requires the knowledge of the direction-of-arrival (DOA) of

[16] In a PN sequence, the transmitted symbols are called *chips*. Also, the PN technique is referred to in the literature as direct sequence spread spectrum (DSSS) technique.

MPCs distribution at the receiver, and the direction-of-departure (DOD) distribution at the transmitter.
Independently of the measuring technique (i.e., narrowband or wideband, and time or frequency domain), the channel parameters estimated from measurements are influenced by the measurement setup, especially by the directional characteristics of the antennas. The influence of the measurement setup is not always easily separable from the CIR.

4.2 Vehicular channel measurement campaigns

Several vehicular channel measurement campaigns have been conducted to investigate the propagation channel characteristics at different environments and frequencies, mainly in the last five years. Table 3 summarizes the most representative measurement campaigns, indicating the frequency, the measuring technique (narrowband or wideband), the type of antennas (SISO[17] refers to a single antenna at the transmitter/receiver, and MIMO refers to multiple antennas at the transmitter/receiver), the propagation link measured (V2V, V2I or V2X) and the environment where the measures were collected. Five types of environments have been considered[18], i.e., urban, suburban, rural, expressway and highway.
The frequency bands correspond to the IEEE 801.11b/g band (2.4 GHz), the IEEE 801.11a band (5.2 GHz) and the DSRC band (5.9 GHz). A study about the channel parameters describing the path loss, as well as the time- and frequency-dispersion behavior will be carried out in Section 5 and 6 of this chapter.

Reference	Frequency	Channel sounder	System configuration	Propagation link	Environment
(Acosta et al., 2004)	2.4 GHz	WB	SISO	V2V	SU, E
(Zajic et al., 2009)	2.4 GHz	WB	MIMO	V2V	H
(Ito et al., 2007)	5.0 GHz	NW	SISO	V2V	U
(Sen & Matolak, 2008)	5.0 GHz	WB	SISO	V2V	U, SU, E, H
(Paier et al., 2007)	5.2 GHz	WB	MIMO	V2X	U, R, H
(Maurer et al., 2002)	5.2 GHz	NB	SISO	V2V	U, SU, E, H
(Renaudin et al., 2009)	5.3 GHz	WB	MIMO	V2V	U, SU, H
(Paschalidis et al., 2008)	5.7 GHz	WB	MIMO	V2V	U
(Acosta & Ingram, 2007)	5.9 GHz	WB	SISO	V2X	U, SU, E
(Cheng et al., 2007)	5.9 GHz	NB	SISO	V2V	SU
(Cheng et al., 2008a)	5.9 GHz	WB	SISO	V2V	SU, R, H
(Tan et al., 2008)	5.9 GHz	WB	SISO	V2X	U, R, H
(Kunisch & Pamp, 2008)	5.9 GHz	WB	SISO	V2V	U, R, H

Table 3. Vehicular channel measurements. NB: Narrowband, WB: Wideband, U: Urban, SU: Suburban, R: Rural, E: Expressway, H: Highway

[17] Single-Input Single-Output.
[18] This is a general classification to facilitate comparisons between empirical results. To know the specific characteristics of the environment where the measurement campaign was conducted, the reader can see the corresponding reference.

5. V2V narrowband channel characterization

Based on the available literature, the most important narrowband parameters of vehicular propagation channels are reviewed in this Section, i.e., path loss, narrowband fading statistics and Doppler spectrum.

5.1 Path loss modeling

Path loss is one of the most important parameters used in the link budget, being a measure of the channel quality. Path loss takes into account all propagation mechanisms that occur in the radio channel, such as free-space, reflection, diffraction and scattering, and is influenced by the propagation environment (e.g., urban, suburban or rural), the directional characteristic and height of the antennas, and the distance between the transmitter and receiver. Path loss is inversely related to the signal-to-noise ratio (SNR), i.e., the higher path loss the lower SNR, thus limiting the coverage area.

Under free space propagation conditions, for a transmitter to receiver separation distance d, the averaged received power in logarithm units (dBm), denoted by $P_R(d)$, is given by the Friis transmission formula as

$$P_R(d) = P_T + G_T + G_R - 10\log\left(4\pi d / \lambda_c\right)^2, \tag{22}$$

where P_T is the transmitted power (in dBm), G_T and G_R are the transmitter and receiver antenna gain (in dBi) in the direction of the propagation wave, and λ_c is the wavelength associated to the carrier frequency f_c. The last term in Eq. (22) represents the path loss for free space propagation conditions, $PL_{FS}(d)$, expressed in decibels (dB) as

$$PL_{FS}(d) = 10\log\left(4\pi d / \lambda_c\right)^2. \tag{23}$$

In different propagation conditions to free space, the path loss expressed in dB, denoted by $PL(d)$, can be expressed in a general way as

$$PL(d) = \overline{PL}(d) + X_\sigma, \tag{24}$$

where $\overline{PL}(d)$ is the average path loss (in dB), and X_σ is a Gaussian random variable with zero mean and standard deviation σ. The X_σ variable accounts for the large-scale fading or shadowing.

In many channel models, the average path loss is proportional to the logarithm of the distance, i.e., $\overline{PL}(d) \propto 10\gamma\log d$, being γ a path loss exponent extracted from channel measured data (from Eq. (23), $\gamma = 2$ in free space).

There are different path loss models proposed in the literature for V2I and V2V propagation links. Next, some path loss models which can be used to vehicular ad hoc networks (VANET) simulations will be presented. In the following, and unless otherwise indicated, path loss will be expressed in dB; distances, antenna heights and wavelength in meters; and frequencies in GHz.

5.1.1 V2I path loss models

Over the last few decades, intense efforts have been carried out to obtain accurate microcell path loss models in dense urban environments. In these models, the transmitting antenna is placed several meters over the streets floor. Nevertheless, only those models which consider the DSRC band can be used to estimate the path loss, as is the case of the microcell urban propagation model developed within the WINNER (Wireless World Initiative New Radio) European Project.

Microcell WINNER path loss model

The model reproduced here corresponds to the extension of the B1 microcell model (WINNER, 2007). This model is based on channel measurement results, considering both LOS and NLOS conditions. The validity frequency range of the model is from 2 to 6 GHz. The model consists of a dual-slope model with and effective height and a *breakpoint* or *critical distance*, denoted by d_c, estimated as

$$d_c = \frac{4h_T^{'}h_R^{'}}{\lambda_c}, \tag{25}$$

where $\lambda_c = c_0 / f_c$ is the wavelength associated to the carrier frequency f_c, $h_T^{'} = h_T - h_0$ and $h_R^{'} = h_R - h_0$, h_T and h_R are the height of the transmitter and receiver antennas, respectively, and h_0 is the effective height due to the presence of vehicles between the transmitter and receiver. h_0 is related to traffic conditions, varying from 0.5 (no or low traffic) to 1.5 (heavy traffic). For moderate traffic $h_0 = 1$. If d is the distance between the transmitter and receiver, the average path loss under LOS conditions is expressed as follows

$$\overline{PL}_{LOS}(d) = \begin{cases} 22.7\log d + 41 + 20\log(f_c / 5), & d < d_c \\ 40\log d + 41 - 17.3\log d_c + 20\log(f_c / 5), & d_c \geq d \end{cases} \tag{26}$$

The maximum range of the model is assumed as several kilometres. For the transmitter and receiver antennas height, the following ranges are proposed: $5\ m < h_T < 20\ m$ and $1.5\ m < h_R < 20\ m$. This model can be applied to V2I links making $h_T = h_{RSU}$ and $h_R = h_{OBU}$ where h_{RSU} and h_{OBU} are the RSU and OBU antenna heights, respectively.
Under NLOS conditions, the average path loss can be expressed as

$$\overline{PL}_{NLOS}(d_1, d_2) = \overline{PL}_{LOS}(d = d_1) + 20 - 12.5n_j + 10n_j \log(d_2), \tag{27}$$

where

$$n_j = \max\{2.8 - 0.0024d_1,\ 1.84\}. \tag{28}$$

The geometry for the microcell WINNER path loss model for NLOS conditions is shown in Fig. 4, where the distances d_1 and d_2 are also illustrated. Eq. (27) is valid for $d_2 > W_S / 2$, being W_S the street width. For $d_2 \leq W_S / 2$ the LOS model can be applied.
According to Eq. (24), the shadowing effect can be modeled by a standard deviation equal to 3 dB for LOS conditions and 4 dB for NLOS conditions.

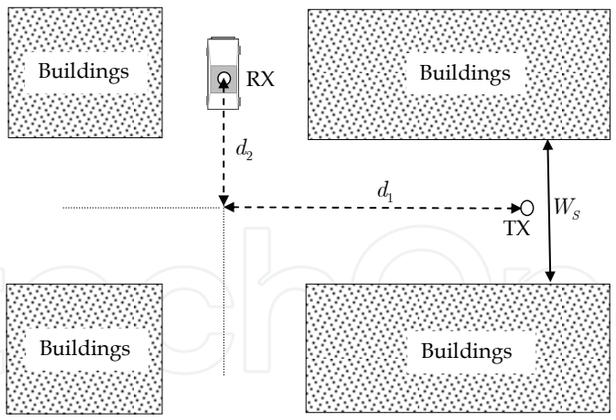

Fig. 4. Geometry for the NLOS WINNER microcell path loss model

5.1.2 V2V path loss models

Differences between V2V and F2M channels oblige the development of new models to estimate the average path loss. Next, we will describe the single- and dual-slope models, indicating the values of their parameters based on different narrowband and wideband channel measurements, as well as the typical two-ray model. Finally, a more elaborated path loss model developed in the University of Kangaku will also be presented.

Single- and dual-slope path loss models

In wireless channel propagation, the conventional single-slope path loss model assumes that the received power decreases with the logarithm of the separation distance between the transmitter and receiver. The average path loss can be estimated as

$$\overline{PL}(d) = \overline{PL}(d_0) + 10\gamma \log(d / d_0), \tag{29}$$

where d is the transmitter to receiver separation distance, $\overline{PL}(d_0)$ is the average path loss for a reference distance d_0, and γ is the well-known propagation path loss exponent. The value of γ takes into account the characteristics of the environment when the propagation occurs. In practice, linear regression techniques based on measured data are used to find the values of the path loss exponent.

However, there are environments where a dual-slope piecewise linear model is able to fit measured data more accurately. A dual-slope model is characterized by a path loss exponent γ_1 and a standard deviation σ_1 above a reference distance up to a breakpoint or critical distance d_c, and by a path loss exponent γ_2 and a standard deviation σ_2 for a distance higher than the critical distance. Using this model, the average path loss can be estimated as

$$\overline{PL}(d) = \begin{cases} \overline{PL}(d_0) + 10\gamma_1 \log(d / d_0), & d_0 \le d \le d_c \\ \overline{PL}(d_0) + 10\gamma_1 \log(d_c / d_0) + 10\gamma_2 \log(d / d_0), & d > d_c \end{cases} \tag{30}$$

In (Green & Hata, 1991), the critical distance d_c is based on the experience and is estimated as $d_c = 2\pi h_T h_R / \lambda_c$, where h_T and h_R are the heights of the transmitter and receiver

antennas, respectively, and being λ_c the wavelength associated to the carrier frequency f_c. Nevertheless, Xia et al. proposed a different critical distance $d_c = 4h_T h_R / \lambda_c$, which is more accurate for V2V links (Xia et al., 1993). However, in practice the critical distance is related to the propagation characteristics environment, and of course, there are important differences among urban, suburban, highway and rural areas. In a similar way as the WINNER path loss model, where an effective height was defined to take into account traffic conditions, Emmelmann et al. have proposed a critical distance $d_c = 4h_T' h_R' / \lambda_c$, with $h_T' = h_T - h_0$, $h_R' = h_R - h_0$, and h_0 being an effective ground offset to model different propagation conditions (Emmelmann et al., 2010). From a measurement campaign at 5.9 GHz in an urban environment, with antennas heights $h_T = 1.51\ m$ and $h_R = 1.93\ m$ at the transmitter and receiver, respectively, a critical distance $d_c = 100\ m$ was derived, resulting in an effective ground offset $h_0 = 0.57\ m$ (Emmelmann et al., 2010).
Table 4 summarizes the values of the path loss exponent and the standard deviations of shadowing derived from channel measurement campaigns conducted in different vehicular environments.

Model	Parameter	Urban	Suburban	Highway	Rural
Single slope	$\gamma / \sigma(dB)$	1.61/3.4 (c)	2.32/7.1 (a) 2.75/5.5 (a)	1.85/3.2 (c)	1.79/3.3 (c)
Dual slope	$\gamma_1 / \sigma_1(dB)$	-	2/5.6 (a) 2.1/2.6 (a)	1.9/2.5 (b)	2.3/3.2 (b)
	$\gamma_2 / \sigma_2(dB)$	-	3.8/4.4 (a) 4/8.4 (a)	4/0.9 (b)	4.0/0.4 (b)
	$d_c(m)$	-	100 (a)	220 (b)	226 (b)

Table 4. Parameters for single- and dual-slope path loss models from different channel measured data: (a) (Cheng et al., 2007), (b) (Cheng et al., 2008b), and (c) (Kunisch & Pamp, 2008)

In addition, a three slope path loss model, with two breakpoints, has been proposed in (CEPT Report 101, 2007), where the first interval of distances considers free-space propagation.

Two-ray path loss model

The two-ray model is widely used in LOS conditions due to its simplicity. According to the classical definition of the two-ray propagation model, the direct path and the reflected wave by the ground can be taken into account to estimate the path loss when there is LOS between the transmitter and the receiver and there are no vehicles between them. The geometry for the two-ray propagation model is illustrated in Fig.5.

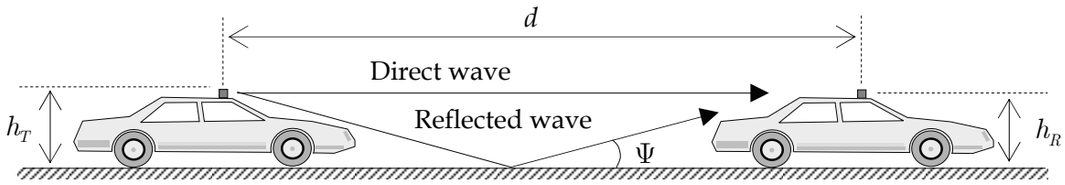

Fig. 5. Geometry for the two-ray propagation model

The superposition of both the direct and the reflected paths at the receiver antenna, results in a fieldstrength gain represented by the term $\left|E_T / E_D\right|$, where E_T and E_D are the total and the direct path fieldstrength at the receiver antenna, respectively. From the geometry given in Fig. 5, the term $\left|E_T / E_D\right|$ can be calculated as follows

$$\left|E_T / E_D\right| = \left|1 + \rho_{\perp,\parallel}(\Psi)\frac{d}{d+\Delta d}\exp(-jk\Delta d)\sqrt{\frac{G_T(\theta_r,\varphi_r)}{G_T(\theta_d,\varphi_d)}\frac{G_R(\theta_r,\varphi_r)}{G_R(\theta_d,\varphi_d)}}\right|, \tag{31}$$

where $\rho_{\perp,\parallel}(\Psi)$ is the Fresnel reflection coefficient of the ground (the street floor in urban environments and the road in expressway and highway environments), for vertical ($\parallel$) or horizontal ($\perp$) polarization, associated to the angle of elevation Ψ; $k = 2\pi/\lambda_c$ is the wavenumber, and Δd is the different between the reflected path and the direct path lengths, that for $h_T, h_R \ll d$ can be estimated as

$$\Delta d \approx 2h_T h_R / d\,. \tag{32}$$

Eq. (31) takes also into account the gain pattern of both the transmitter and the receiver antennas, $G_T(\theta,\varphi)$ and $G_R(\theta,\varphi)$, respectively, with (θ_d,φ_d) and (θ_r,φ_r) being the angular directions associated to the direct and reflected paths, respectively.

Eq. (31) corresponds to a rigorous evaluation of the interference between the direct and the reflected paths, that must be taken into account for short-ranges, i.e., when the distance d is comparable with the antennas heights h_T and h_R. However, for large-ranges, i.e., when $d \gg h_T, h_R$, the following simplifications can be applied: (1) the elevation angle, Ψ in Fig.5, is close to 0 (grazing incidence), (2) $\rho_{\perp,\parallel}(\Psi \to 0) \approx -1$, and (3) $G_T(\theta_d,\varphi_d) \approx G_T(\theta_r,\varphi_r)$ and $G_R(\theta_d,\varphi_d) \approx G_R(\theta_r,\varphi_r)$. Thus, Eq. (31) can be simplified and rewritten as

$$\left|E_T / E_D\right| \approx \left|1 - \exp(-jk\Delta d)\right| = \left|2\sin(\pi\Delta d/\lambda_c)\right|_{\Delta d \approx 2h_T h_R/d} \approx \left|2\sin\left(\frac{2\pi h_T h_R}{\lambda_c d}\right)\right|. \tag{33}$$

The term $\left|E_T / E_D\right|$ derived from Eq. (33) is shown in Fig.6 (a), for typical antennas heights in V2V communications ($h_T = h_R = 1.75$ m) and $\rho_{\parallel,\perp} = -1$.

For small distances between the transmitter and the receiver, the influence of the interference between the direct and the reflected paths is visible, and $\left|E_T / E_D\right|$ undergoes space fading until a breakpoint distance or critical distance given by $d_c = 4h_T h_R/\lambda_c$. It is worth noting that the maximum value (6 dB) of the term $\left|E_T / E_D\right|$ occurs for a distance where the interference of the reflected path is totally constructive; whereas the minimum value is obtained for a distance where the interference is totally destructive.

When the two-ray propagation model is considered, the Friis transmission formula given by Eq. (22), is reedited as follows

$$P_R(d) = P_T + G_T(\theta_d,\varphi_d) + G_R(\theta_d,\varphi_d) - PL_{FS}(d) + 10\log\left|E_T / E_D\right|^2, \tag{34}$$

being the total two-ray path loss of the link

$$PL(d) \triangleq 10\log(4\pi d/\lambda_c)^2 - 10\log\left|E_T / E_D\right|^2. \tag{35}$$

Fig.6 (b) shows the total path loss versus the transmitter to receiver separation distance, where $h_T = h_R = 1.75$ m and $\rho_{\parallel,\perp} = -1$ have been considered.

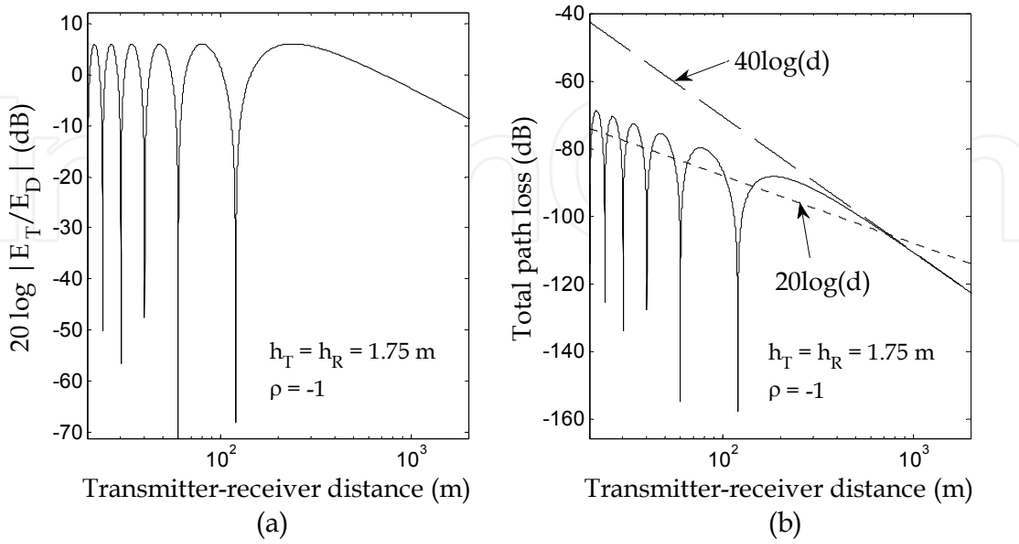

Fig. 6. Two-ray propagation model: (a) interference between the direct and the reflected paths, and (b) total path loss

Measurement results reported in the Reference (Kunisch & Pamp, 2008), show that the two-ray propagation model can be used in highway and rural environments. Due to the direct path can be affected by the surrounding environment, Kunisch and Pamp suggest an average path loss, denoted here by $\overline{PL}_{Two-ray}(d)$, in the way of

$$\overline{PL}_{Two-ray}(d) = PL_0 + 10\gamma \log d - 10\log\left|E_T / E_D\right|^2, \tag{36}$$

where γ is a path loss exponent different from 2 (LOS conditions), and PL_0 is a constant. Both γ and PL_0 can be extracted from measured data using linear regression techniques. When $\Delta d \ll \lambda_c$, Eq. (33) can be simplified once again and rewritten as

$$\left|E_T / E_D\right| \approx 2\frac{2\pi h_T h_R}{\lambda_c d}. \tag{37}$$

Then, the total average path loss is given by

$$PL(d) \approx 10\log\left(\frac{4\pi d}{\lambda_c}\right)^2 - 10\log\left(\frac{4\pi h_T h_R}{\lambda_c d}\right)^2 = 10\log\left(\frac{d^2}{h_T h_R}\right)^2, \tag{38}$$

yielding to the well-known d^4 power law, i.e., the total path loss is proportional to the fourth power of the transmitter to receiver separation distance.

Kangaku University model

Based on channel measurements, a prediction formula to estimate the average path loss in urban environments, with both LOS and NLOS conditions, was proposed in (Ito et al., 2007).

The average path loss under LOS conditions is estimated as follows

$$\overline{PL}_{LOS} = \left[10.4 + 1.3\log\left(\frac{h_T h_R}{\lambda_c}\right)\right]\log d + 24.6\log\left(1 + \frac{d}{d_c}\right) + 19.4\log f_c + 3.9\log W_S + 33\,, \quad (39)$$

where f_c is the carrier frequency; d_c is a critical distance estimated by $d_c \approx 8h_T h_R / \lambda_c$; and W_s is the street width. The geometry of the path loss model for LOS conditions is shown in Fig. 7. Table 5 summarizes the validity range of Eq. (39).

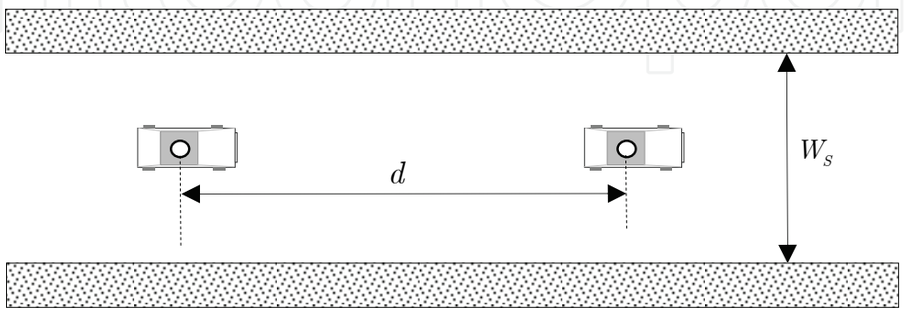

Fig. 7. Geometry of the Kangaku University path loss model for LOS conditions (Ito et al., 2007)

Parameter	Urban environment
$d(m)$	2-1000
$f_c(GHz)$	0.4-6
$W_S(m)$	8, 20, 40, 60
$h_T, h_R(m)$	0.5-3.5

Table 5. Applicable range of the Kangaku University LOS model

For NLOS conditions, the model considers the geometry and parameters illustrated in Fig. 8. The average path loss is estimated as follows

$$\overline{PL}_{NLOS} = \begin{cases} \overline{PL}_{LOS}, & D \le d_{EL} \\ \min\left(\overline{PL}_{NLOS\text{-}1}, \overline{PL}_{NLOS\text{-}2}\right), & D > d_{EL} \end{cases} \quad (40)$$

where

$$D = d_1 + W_{S1} + W_{S2} + d_2\,, \quad (41)$$

$$d_{EL} = d_1 + W_{S1} + W_{S2} + \left(W_{S1}W_{S2} / d_1\right), \quad (42)$$

and

$$\overline{PL}_{NLOS\text{-}1} = \left\{\left(3.2 - 0.033W_1 - 0.022W_2\right)d_1 + 39.4\right\}\left\{\log\left(D\right) - \log\left(d_{EL}\right)\right\} + L_{LOS}\left(d_{EL}\right), \quad (43)$$

$$\overline{PL}_{NLOS\text{-}2} = \left\{-6.7 + 11.2\log\left(\frac{h_T h_R}{\lambda_c}\right)\right\}\log(D) + \left\{25.9 + 10.1\log\left(\frac{d_1}{\lambda_c}\right)\right\}\log\left(1 + \frac{D}{d_c}\right) + 19.8\log(f_c) - 3.8\log(W_1 W_2) + 57.7 \quad (44)$$

with $d_c = 4h_T h_R / \lambda_c$ being the critical distance.
However, a new modification which improves the prediction of path loss has been proposed in (Sai et al., 2009), for both LOS and NLOS conditions, where the average path loss given by Eqs. (39) and (44) are substituted by the following expressions

$$\overline{PL}_{LOS} = \left[7.2 + 7.1\log\left(\frac{h_T h_R}{\lambda_c}\right)\right]\log(D') + 28.3\log\left(1 + \frac{D'}{d_c}\right) - 1.2\log(f_c) - 19.6\log(W_s) + 65.9 \quad (45)$$

$$\overline{PL}_{NLOS-2} = \left\{47.6 + 6.6\log\left(\frac{h_T h_R}{\lambda_c}\right)\right\}\log(D') + \left\{89.1 - 33\log\left(\frac{d_1}{\lambda_c}\right)\right\}\log\left(1 + \frac{D'}{d_c}\right) + 19.9\log(f_c) - 11.3\log(W_1 W_2) + 2.8 \quad (46)$$

with $D' = d_1 + d_2$. Eqs. (45) and (46) were adjusted from measurement results under real traffic conditions.

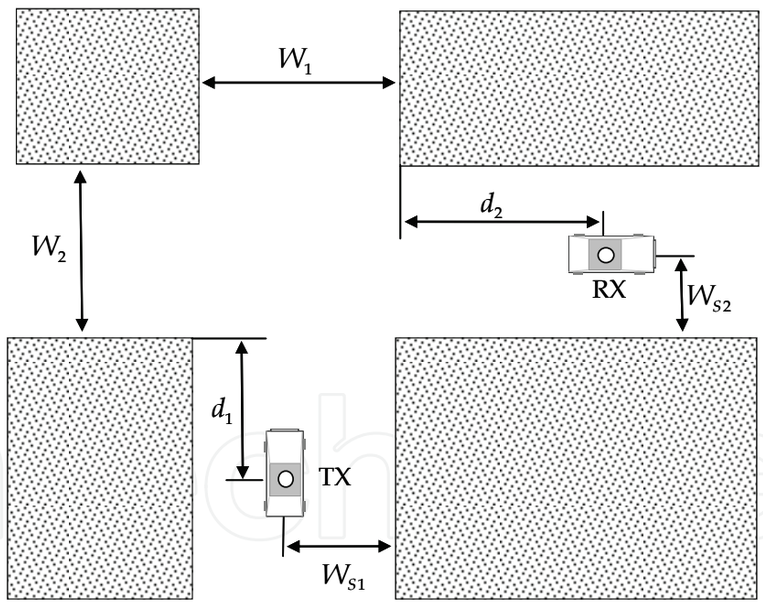

Fig. 8. Geometry of the Kangaku University path loss model for NLOS conditions (Sai et al., 2009)

5.2 Narrowband fading statistics

In a time-variant channel, the multipath propagation causes signal fading due to the phase differences among the MPCs. This signal fading, referred to as small-scale fading, can be modeled by the classical Rayleigh and Rice distributions. Rayleigh fading occurs when the number of MPCs is high having similar amplitudes. From the central limit theorem (CLT),

the time variation of the received signal enveloped, denoted by $r(t)$, in a small local area around the receiver follows a Rayleigh distribution, with probability density function (pdf) given by

$$pdf_r(r) = \frac{r}{\sigma^2}\exp\left(-\frac{r^2}{2\sigma^2}\right), \tag{47}$$

where $E\{r^2\} = 2\sigma^2$ is the mean square value of the distribution, equivalent to the average power of the received signal. Rayleigh fading occurs generally in NLOS conditions. Whereas, in LOS conditions where a dominant contribution with a power A^2 exists, the received envelop follows a Rice distribution, given by

$$pdf_r(r) = \frac{r}{\sigma^2}\exp\left(-\frac{r^2 + A^2}{2\sigma^2}\right) I_0\left(\frac{rA}{\sigma^2}\right), \tag{48}$$

where $I_0(\cdot)$ is the zeroth-order modified Bessel function of the first kind (Gradsthteyn & Ryzhik [8.406], 2007). The mean square value of the Rice distribution is $E\{r^2\} = 2\sigma^2 + A^2$. To model the severity of fading, it is common to use the so-called Rice K factor defined as the relation between the power of the dominant contribution and the power associated to the diffuse MPCs, i.e.

$$K \triangleq \frac{A^2}{2\sigma^2}. \tag{49}$$

Note that when $K \to 0$, the Rice distribution tends to the Rayleigh distribution (Eq. (48) $\to$ Eq. (47)). Ricean fading occurs generally in LOS conditions. Based on measured data, other distributions have been applied to model the small-scale fading, such as the Nakagami-*m* and Weibull distributions. In Nakagami-*m* fading, the pdf of the received signal envelope is given by

$$pdf_r(r) = \frac{2}{\Gamma(m)}\left(\frac{m}{\Omega}\right)^m r^{2m-1}\exp\left(-\frac{m}{\Omega}r^2\right), \tag{50}$$

where $\Omega = E\{r^2\}$ and m is the so-called *shape factor* (fading parameter). When $m = 1$, the Nakagami-*m* distribution yields the Rayleigh distribution (note that $\Omega = 2\sigma^2$), and if $m \gg 1$ the Nakagami-*m* distribution can approximate the Rice distribution, with (Molisch, 2005)

$$\Omega = 2\sigma^2 + A^2 \tag{51}$$

$$m\big|_{m\gg 1} \approx (K+1)^2 / (2K+1). \tag{52}$$

In Weibull fading, the pdf of the received signal envelope is given by

$$pdf_r(r) = \frac{\beta}{\Omega} r^{\beta-1}\exp\left(-\frac{r^\beta}{\Omega}\right), \tag{53}$$

where $\beta > 0$ is the fading parameter. When $\beta = 2$, the Weibull distribution yields the Rayleigh distribution, and if $\beta \gg 2$ the Weibull distribution can also approximate the Rice distribution.

Measured results in urban and highway environments reported in (Maurer et al., 2002) show that small-scale fading can be approximated very well by the Rice and Nakagami-*m* distributions. Also, in (Cheng et al., 2007) the observed trend is a good match with the Rice distribution for short transmitter-receiver separation distances, whereas for large distances the small-scale fading is better modeled using the Rayleigh distribution. Nevertheless, there are situations of large distances, where the Nakagami-*m* distribution offers a better fit to the measured data, caused by an intermittent loss of the dominant MPC at large distances, e.g. when the transmitter and receiver are separated around corners. In (Cheng et al., 2007) based on two data sets, high values of m between 3 and 4 have been estimated from short transmitter to receiver distances (approximately less than 4.5 m), whereas for large distances $m < 1$ (e.g. $m = 0.45$ for distances ranging from 71 m to 177 m), indicating fading more severe than Rayleigh.

Regarding to the large-scale fading or shadowing, produced by the obstruction of MPCs, measured results reported in (Maurer et al., 2002) show that it can be well approximated by a log-normal distribution. Nevertheless, there are situations in which an intermittent blockage of the MPCs exists, causing that the random variable X_σ in Eq.(24) not follow a Gaussian distribution. In this latter case, based on empirical results Cheng et al. proposed to jointly model the small- and large-scale fading using the Nakagami-*m* distribution (Cheng et al., 2007).

5.3 Doppler spectrum

The channel variability over time and the multipath propagation effect cause frequency dispersion or Doppler spread. The movement of both the transmitter and receiver terminals, as well as the interacting objects, e.g. other vehicles between the terminals, make that the Doppler spread to be different to the conventional F2M systems. Theoretical Doppler spectrum models and experimental results are presented in this Subsection.

5.3.1 Theoretical models

The first theoretical approach of the Doppler spectrum in a V2V channel was based mainly on two important assumptions: (1) both the angle-of-departure (AOD) and the angle-of-arrival (AOA) of MPCs are uniformly distributed over (0, 2π[, and (2) the CIR has a uniform power profile. The above assumptions yield the isotropic scattering assumption, and thus the Doppler PDS, $P_H(\nu)$, is given by (Akki & Haber, 1986)

$$P_H(\nu) = \begin{cases} \dfrac{1}{\pi^2 \nu_R \sqrt{a}} K\left[\dfrac{(1+a)}{2\sqrt{a}} \sqrt{1 - \left(\dfrac{\nu}{(1+a)\nu_R}\right)^2}\right] & -(\nu_T + \nu_R) < \nu < \nu_T + \nu_R \\ 0 & \text{otherwise} \end{cases}, \tag{54}$$

where $a = \nu_T / \nu_R$; $\nu_T = v_T / \lambda_c$ and $\nu_R = v_R / \lambda_c$ are the maximum Doppler frequencies of the transmitter and receiver, respectively, being v_T and v_R the transmitter and receiver

speed, respectively, and λ_c the wavelength; and $K[\cdot]$ is the complete elliptic integral of the first kind (Gradsthteyn & Ryzhik [8.112 1], 2007). Fig. 9 shows the behavior of the Doppler PDS as a function of the frequency, for different values of a.

When $a=0$, the maximum Doppler frequency of the transmitter is null and therefore, the transmitter is static, which corresponds to a V2I channel. In this case, Eq. (54) can be simplified an rewritten as follows

$$P_H(\nu)=\begin{cases}\dfrac{1}{\pi\nu_R\sqrt{1-\left(\dfrac{\nu}{\nu_R}\right)^2}} & -\nu_R<\nu<\nu_R \\ 0 & \text{otherwise}\end{cases}, \tag{55}$$

which is the classical Jakes Doppler PDS (Clark, 1968), (Jakes, 1974). From Eq. (54), the *rms* Doppler spread can be calculated as

$$\nu_{rms}=\left(\frac{1}{\lambda\sqrt{2}}\right)v_{eff}=\left(\frac{1}{\lambda}\right)\sqrt{\frac{v_T^2+v_R^2}{2}}, \tag{56}$$

where $v_{eff}\triangleq\sqrt{v_T^2+v_R^2}$ is defined as the effective speed (Cheng et al., 2007). For non-isotropic scattering channels, i.e. non uniform distribution of both AOD and AOA, a general closed form for the $P_H(\nu)$ has not been obtained. However, simulation results of the PDS show that in a non-isotropic channel the Doppler PDS exhibits one-sided Doppler shifts (Zheng, 2006).

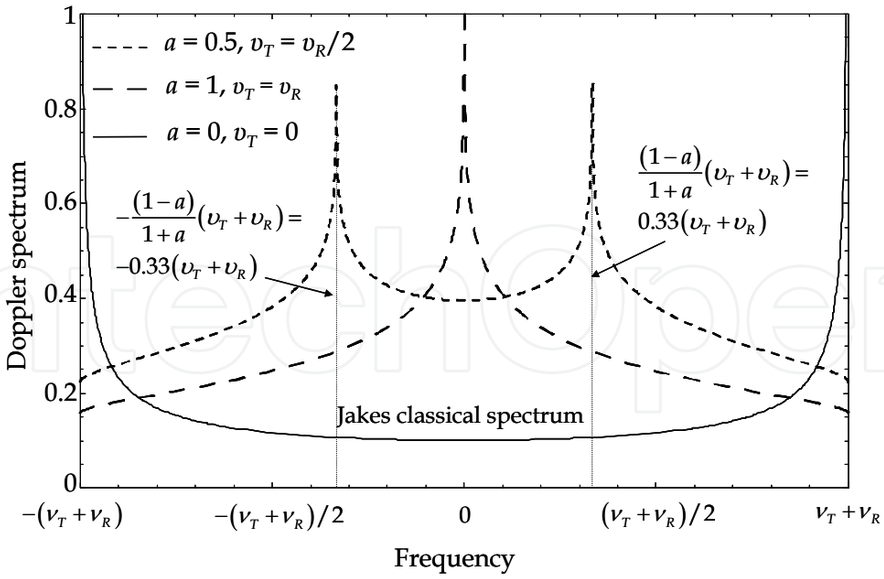

Fig. 9. Normalized Doppler PDS for the V2V channel (Akki & Habber, 1986)

Nevertheless, for a V2V specific scenario in an urban canyon, where there are two dense reflectors located along one side of the road as shown in the Fig. 10(a), the Doppler PDS can be estimated as (Jiang et al., 2010)

$$P_H(\xi)=\begin{cases}\dfrac{1}{A\nu_d}\dfrac{1}{\sqrt{1-\xi^2}}\times\left\{\left[\dfrac{d_2}{\sqrt{1-\xi^2}}+\sqrt{\left(d_0-\dfrac{d_2}{\xi}\sqrt{1-\xi^2}\right)^2+d_1^2}\right]^{-\gamma}\right. & \\ \left.+\left[\dfrac{d_2'}{\sqrt{1-\xi^2}}+\sqrt{\left(d_0-\dfrac{d_2'}{\xi}\sqrt{1-\xi^2}\right)^2+d_1'^2}\right]^{-\gamma}\right\} & -1\le\xi\le 1 \\ 0 & \text{otherwise}\end{cases}, \tag{57}$$

where $\xi=\nu/\nu_d$; $\nu_d=v_d/\lambda_c$, being v_d the relative speed between vehicles, d_0 is the distance between the transmitter and receiver along the road; d_1' and d_2' are the distances illustrated in Fig. 10(a); γ is the path loss exponent; and

$$A=\int_{-\pi}^{0}\frac{1}{(r')^{\gamma}}d\beta+\int_{0}^{\pi}\frac{1}{r^{\gamma}}d\alpha\,, \tag{58}$$

with

$$r=r_1+r_2=\sqrt{\left(d_0-\frac{d_2\cos\alpha}{\sin\alpha}\right)^2+d_1^2}+\frac{d_2}{\sin\alpha}\,, \tag{59}$$

$$r'=r_1'+r_2'=\sqrt{\left(d_0-\frac{d_2'\cos\beta}{\sin\beta}\right)^2+d_1'^2}+\frac{d_2'}{|\sin\beta|}\,, \tag{60}$$

where $|\cdot|$ denotes absolute value.

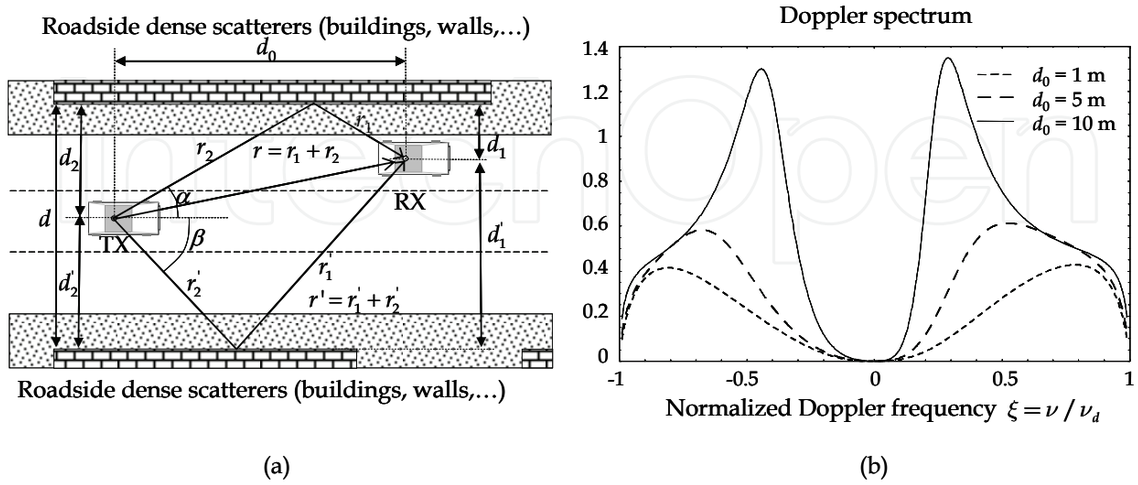

(a) (b)

Fig. 10. (a) Illustration of a typical urban canyon environment and (b) its corresponding Doppler PDS, when $d_1=d_2'=3\ m$, $d_2=d_1'=5\ m$ and $\gamma=3$ (Jiang et al., 2010)

For distances along the road, d_0, with similar order of magnitude to the distances d_1, d_2, $d_1^{'}$ and $d_2^{'}$ shown in Fig. 10(a), the curves are smoothed and the asymptotes of Fig. 10(b) do not appear. Otherwise, for asymmetrical positions of vehicles, i.e. $d_1 \neq d_2^{'}$ and $d_2 \neq d_1^{'}$, the asymmetry of the Doppler PDS increases around the central Doppler frequency.

5.3.2 Experimental results

The *rms* Doppler spread derived from different measurement campaigns, (Cheng et al., 2007), (Cheng et al., 2008c) can be approximated as a function of the effective speed, v_{eff}, by

$$\nu_{rms} = \frac{s}{\lambda_c \sqrt{2}} v_{eff} + \delta \,, \tag{61}$$

where $s / \lambda_c \sqrt{2}$ is the slope and δ is an offset. Note that according to Eq. (56), $s = 1$ and $\delta = 0$ for isotropic scattering. Table 6 summarizes the values of s and δ for highway, rural and suburban V2V environments (Cheng et al., 2008c).

Parameter	Suburban	Highway	Rural
Offset, δ	11.2	0.2	0.5
s	0.428	0.414	0.420

Table 6. Parameters measured of *rms* Doppler spread

It should be emphasized that s is significantly less than 1 due to the non-isotropically oriented scattering objects in real scenarios.

Likewise, it can be seen that the Doppler spread usually increases if the transmitter to receiver distance grows. Obviously, this spreading is the result of the tendency for the vehicle speeds to be higher at larger distances. In situations of platoon, since the average relative velocity between the vehicles is close to zero, it is comprehensible that the average Doppler spread, $\overline{\nu}$, is approximately 0.

Table 7 summarizes the results of Doppler parameters for a platoon of vehicles, with a distance between transmitter and receiver ranging from 5 to 300 m, under realistic traffic conditions.

Parameter	Urban	Highway
$\overline{\nu}$	2.03 Hz	0.93 Hz
ν_{rms}	85.6 Hz	119.98 Hz

Table 7. Doppler spectrum parameters measured under platoon conditions, from (Maurer et al., 2002)

5.3.3 Coherence time

The coherence time has an inverse relation to the *rms* Doppler spread. The coherence time can be related to the *rms* Doppler spread in terms of a proportionality *k*-constant

$$T_C \approx k / \nu_{rms} \,, \tag{62}$$

where k represents the time correlation degree. In a V2I channel, k can be analytically derived. For a time correlation degree greater than 50%, $k_{>50\%} \approx 9/\left(16\sqrt{2}\right)\pi$ (Sklar, 1997).

According to (Cheng et al., 2007), in a V2V channel an estimation of k for a correlation degree equal to 90% is $k_{90\%} \approx 0.3$.
From Eq. (61) and Eq. (62), the coherence time has an inverse relationship to the effective speed. Also, results reported in (Cheng et al., 2007) show that the coherence time decreases as the distance between transmitter and receiver grows.

6. V2V wideband channel characterization

This Section provides a brief wideband channel description based on channel data collected in the measurement campaigns summarized in the Table 3. It is worth noting that the measurement results published in the literature have shown that the propagation characteristics are closely related to the type of environment, and in similar environments with different frequencies can also vary significantly. For this reason, the metric values reported here will be applicable for environments with similar characteristics as those where the measurements were collected.

6.1 V2V TDL channel model

In channel modeling, the most popular wideband model is the TDL channel model. The CIR of a TDL channel model of *N* taps is written as

$$h(t,\tau) = \sum_{i=1}^{N} h_i(t)\delta(\tau - i\Delta\tau), \tag{63}$$

where $\Delta\tau = 1/B$, being B the channel bandwidth[19]. A first approximation to the total number of taps can be derived from the *rms* delay spread as

$$N \simeq \left\lceil \frac{\tau_{rms}}{\Delta\tau} \right\rceil + 1, \tag{64}$$

where $\lceil \cdot \rceil$ represents the nearest upper integer function. A TDL channel model should describe the number of taps, the relative taps power, the fading amplitude statistics and the Doppler PDS for each tap. Some V2V TDL channel models have been published in the literature (Acosta & Ingram, 2007), (Sen & Matolak et al., 2008), (Renaudin et al., 2009) and (Wu et al., 2010). The reader is referred to those references in order to have a better knowledge of how the models have been built.
The tap fading amplitude statistics can be described by the well-known Rayleigh or Rice distributions, as is the case of the model proposed in (Acosta & Ingram, 2007). Nevertheless, other researchers have found a better fit to the measured results through the Nakagami-*m* and Weibull distributions. Different small-scale fading conditions have been observed for a given tap, ranging from Rician fading (equivalent to fading parameters $m > 1$ and $\beta > 2$ for the Nakagami-*m* and Weibull distributions, respectively) to more severe than Rayleigh fading (equivalent to $m < 1$ and $\beta < 2$). In (Renaudin et al., 2009), the fading parameter β takes values from 1.56 to 3.75. In (Sen & Matolak. 2008) the best fit to the measurements is performed using the Weibull distribution, where the values of β oscillates from 1.29 to 5.15.

[19] When a correlative channel sounder is use to estimate the CIR, *B* is equal to the inverse of the time resolution.

In (Wu et al., 2010), as an extension work of (Sen & Matolak. 2008), additional TDL channel models are provided in terms of the channel bandwidth, where the tap fading statistics is also modeled by the Weibull distribution, with β ranging from 1.59 to 4.97 for a channel bandwidth of 20 MHz.

6.2 RMS delay spread

Statistical values of the *rms* delay spread and maximum delays have been reported in the literature based on measurement campaigns. In (Kunisch et al., 2008) values of *rms* delay spread equal to 52 ns, 41 ns and 47 ns were estimated for rural, highway and urban areas, respectively, for a maximum transmitter-receiver separation of about 300 m. Whereas, in (Tan et al., 2008) higher values have been estimated for the same transmitter-receiver separation. Table 8 summarizes the *rms* delay spread values reported in (Tan et al., 2008) for different environments, vehicles distances and propagation conditions (LOS and NLOS).

	LOS	NLOS
Rural (100 m)	21.6	-
Highway (300 m)	156.8	-
Highway (400 m)	141.8	398
Urban (200 m	157.5	295
Urban (400 m)	320.6	-
Urban (600 m)	286.6	-

Table 8. RMS delay spread vales, in ns, for different environments and transmitter-receiver separation distances, from (Tan et al., 2008)

Values of *rms* delay spread reported in (Sen & Matolack, 2008) take into account the location position of the antenna and the VTD. Thus, 256 ns has been estimated in urban environments with the antenna outside the car, and 125.8 ns with the antenna inside the car. For open areas, the values reported are 53.2 ns and 126.8 ns for low and high traffic conditions respectively.

In (Cheng et al., 2008a), a comparative study of the time- and frequency-dispersion behavior was performed. Values of maximum delay spread of 0.6 μs, 1.4 μs and 1.5 μs was estimated for suburban, highway and rural areas, respectively. These values correspond to a 90% probability, i.e., values which can be observed in the 90% of times or situations. For a correlation degree equal to 90%, the following coherence bandwidths have been estimated: 730 kHz, 520 kHz and 460 kHz for suburban, rural and highway areas, respectively.

In general, vehicular environments are mainly characterized by the presence of local interacting objects and the longest delay spread appears in canyon scenarios under NLOS conditions, i.e., street canyons in urban areas and highway environments when big vehicles exist in the transmitter and receiver proximity. This is a further difference with respect to cellular systems, where the longest time dispersion occurs within open and suburban areas.

6.3 RMS Doppler spread

As started in the previous Section, in V2V channels the Doppler PDS can differ to the classical U-shaped spectrum due to the AOA of MPCs has a non-uniform distribution. Values of the *rms* Doppler spread reported in the literature are clearly dependent on the vehicular speed used in the measurement campaign. Values of *rms* Doppler spread less than

1 kHz have been measured. These values are a small fraction of the inter-carrier frequency defined in IEEE 802.11p (156.25 kHz), indicating that the Doppler spread may not cause significant inter-carrier interference (ICI). Nevertheless, the coherence time in vehicular environments can introduce impairments when long symbol packets are transmitted.
Based on channel measurements, in (Acosta & Ingram, 2007) different Doppler PDS shapes for each tap of the TDL channel model are provided: flat, round, classic 3 dB and classic 6 dB.

7. Some aspects related to the antennas for vehicular communications

Both the infrastructure and the vehicle antennas in the ITS 5.9 GHz band are typically directive in the vertical plane and omni-directional in the azimuth plane. The antennas in vehicles are usually mounted either on the roof or inside the vehicle (e.g. under the windshield, in rear view mirror, on a seat or near a dashboard) although some vehicles can have additional antennas for radar applications in the bumper. For instance, the antennas are usually mounted under the windshield of the vehicle, inside the device known as tag or on-board equipment (OBE), for toll collection applications and parking control working in the CEN DSRC 5.8 GHz band (CEN EN 12253, 2004).
The effect of the antenna placement in vehicles is significant (Kaul et al., 2007). The differences in the cumulative link packet error rates are until 25-30% depending on the antenna locations under LOS conditions. Gain patterns of omni-directional antennas in the azimuth plane become asymmetric in certain positions of the vehicle, showing only an accurate approximation to the omni-directional pattern if the antenna is mounted on the center of the vehicle roof.
The antenna can be designed as either wideband dipole antenna (Chen et al., 2005) or double-fed printed monopole (Jensen et al., 2007) for OBU, and double-looped monopole (Kim et al., 2003) for RSU, operating in WLAN 2.4-2.485 GHz, 5.47-5.725 GHz and ITS 5.9 GHz bands.
The antenna radiation pattern in the vertical plane can be approximated using the ITU-R F.1336 Recommendation (CEPT Report 101, 2007), (ITU-R F.1336, 2007), where the gain, expressed in dBi, for an elevation angle θ_1 is given by

$$G(\theta) = \max\left[G_1(\theta), G_2(\theta)\right], \tag{65}$$

with

$$G_1(\theta) = G_0 - 12\left(\frac{|\theta - \theta_1|}{\Delta\theta_{-3dB}}\right)^2, \tag{66}$$

$$G_2(\theta) = G_0 - 15 + 10\log\left[\left(\max\left\{\frac{|\theta - \theta_1|}{\Delta\theta_{-3dB}}, 1\right\}\right)^{-1.5} + k\right], \tag{67}$$

where θ_1 is the tilt of the gain elevation pattern; $\Delta\theta_{-3dB}$ is the -3 dB beamwidth in the vertical plane $\Delta\theta_{-3dB} = 107.6 \times 10^{-0.1\,G_0}$, being G_0 the maximum gain (in dBi); and $k = 0$ is the sidelobe factor for the frequency range from 3 GHz to 70 GHz. All angles in Eqs.(65)-(67) are expressed in degrees.

Fig. 11(a) shows an example of the approximated gain pattern in the vertical plane for a vehicle antenna using Eqs.(65)-(67). Maximum gains of 5 and 8 dBi have been considered. In Fig. 11(b), the main parameters of the RSU and OBU antennas are illustrated. The height and the tilt of the RSU antenna depend on the range of the transmission. Regardless RSU antenna, the height is limited to 15 m above the road surface. For applications in CEN DSRC 5.8 GHz band (CEN EN 12253, 2004), the antenna height is around 5.5 m, with a usual antenna tilt of 55º; and for larger-range applications in the ITS 5.9 GHz band the typical RSU antenna elevation is about 6 m with an antenna tilt equal to 45º.

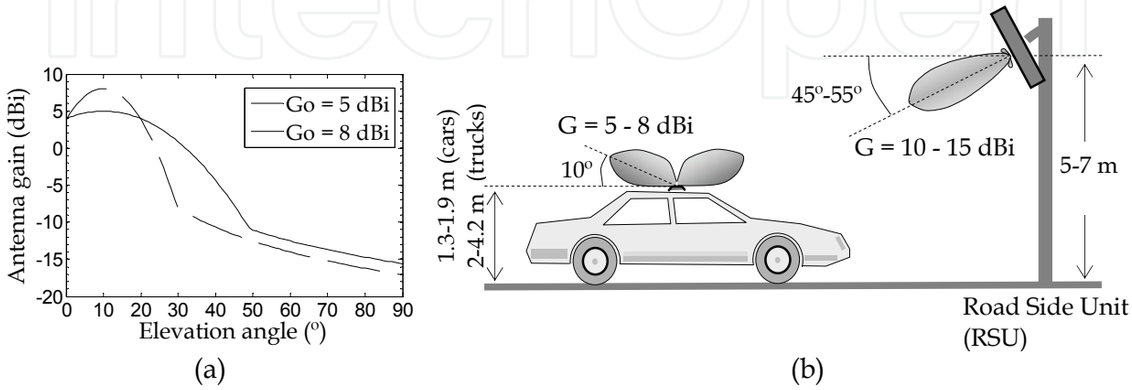

Fig. 11. (a) Gain pattern in the vertical plane for the ITS 5.9 GHz band, with maximum gains of 5 and 8 dBi, and (b) antenna installation in the vehicle and in the RSU for ITS applications at 5.9 GHz

8. Future advances in channel modeling for vehicular communications

Although advances have been made within V2V channel modeling, there are still many remaining unanswered questions. Further empirical studies should be conducted to improve the accuracy of channel models, considering the possible combinations of real propagation conditions. For this purpose, more measurement campaigns covering a greater variety of scatterers density, vehicles speed, LOS and NLOS conditions, are necessary. In this sense, the future challenges should be oriented to channel measurements and the development of parameterized channel models, where the main channel parameters estimated from real data could be introduced in the channel model.

The Doppler PDS is an important parameter which characterizes the frequency-dispersion behavior of vehicular environments. In order to develop more accurate channel models based on the TDL concept, further studies of non-isotropic scattering based on measurements should be conducted. In addition, the transmitter and receiver direction of motion affect the channel parameters. Few measurement campaigns have considered the transmitter and receiver moving in opposite directions, especially in expressways and highways, where the vehicles speed is high. In this sense, more measurement campaign should be conducted when the transmitter and receiver are moving in opposite directions and for various vehicular traffic densities in different environments.

The measurement campaigns performed consider short separation distances between the transmitter and the receiver, with a maximum distance of about 400 m. Although there are still few applications involving vehicles separated by large distances, measurement

campaigns are required to explore the propagation characteristics for large ranges, e.g., larger than 1 km.
In the measurement campaigns, the antennas are placed in elevated positions of the vehicles. Since the antenna position in the vehicle can affect the packet error rate, other vehicles positions, near to real implementations, should be considered. Also, the typical vehicles involved in the measurements are vans. More measurements are necessary considering a greater variety of vehicles, since the propagation mechanisms, especially the obstruction effects, are related to the height of the antennas.
Exploring the available literature, little attention has been devoted to V2I measurement campaigns compared with the V2V case. Since some safety applications involve RSUs, more measurements of the V2I channel are required, developing more realistic channel models. It is also interesting to obtain V2I path loss models for highway and rural areas taking into account the effective height of the terrain, as well as the road curves and other important interacting objects that comprise the propagation environment.
Other frequency bands, as the low part of the UHF band may be also allocated to V2V communications. In Japan, a 10 MHz band from 715 MHz to 725 MHz has been already assigned for ITS applications to prevent oncoming traffic collisions (Sai et al., 2009). It is interesting to explore the propagation characteristics at these frequencies, because significant differences to the 5.9 GHz band exist.
Finally, since large differences exist among cities, expressways and highways around the world, to have a better knowledge of the vehicular channel propagation characteristics in specific environments more measurement campaigns must be conducted in different places.

9. Conclusions

The ITS concept for DSRC systems, together with new applications related to driving safety and mobile ad hoc networks, have triggered great interest in vehicular channel modeling during the last decade, and specially in the five last years. Differences between vehicular and traditional cellular channels require new channel models and measurement campaigns to understand the signal impairments introduced by the time- and frequency-dispersive behaviour of the vehicular channel. The main characteristics of vehicular environments, make that the vehicular channel have great incidence to the final system performance. As mentioned, an accurate knowledge of the vehicular channel is vital to implement safety applications.
In this Chapter, principal propagation aspects in vehicular networks have been analyzed. Based on the available literature, an overview of V2V and V2I channel modeling and channel measurements has been reported. A narrowband characterization of the V2V and V2I channel has been made, where the most important path loss and Doppler PDS models have been described. Also, information of wideband channel parameters has been provided. Finally, future advances in channel modeling for vehicular communications have been identified.

10. References

Acosta-Marum, G. & Ingram, M. A. (2007). Six time- and frequency-selective empirical channel models for vehicular wireless LANs. *IEEE Vehicular Technology Magazine*, Vol. 2, No. 4, pp. 4-11.

Acosta-Marum, G.; Tokuda, K. & Ingram, M. A. (2004). Measured joint Doppler-delay power profiles for vehicle-to-vehicle communications at 2.4 GHz. *IEEE Global Telecommunications Conference*, Vol. 6, pp. 3813-3817, Atlanta, GA, Dec. 2004.

Akki, A. S. & Haber, F. (1986). A statistical model for mobile-to-mobile land communication channel. *IEEE Transactions on Vehicular Technology*, Vol. 35, No. 1, pp. 2-7.

Akki, A. S. (1994). Statistical properties of mobile-to-mobile land communication. *IEEE Transactions on Vehicular Technology*, Vol. 43, No. 4, pp. 826-836.

Almalag, M. S. (2009). *Vehicular Networks : from Theory to Practice,* Olariu, S. & Weigle, M. C. , Ed., pp. 5.1-5.26, Chapman & Hall/CRC Press, Boca Raton, FL, USA.

Almers, P.; Bonek, E.; Burr, A.; Czink, N.; Debbah, M.; Degli-Esposti, V.; Hofstetter, H.; Kyösty, P.; Laurenson, D.; Matz, G.; Molisch, A. F.; Oestges, C. & Özcelik, H. (2007). Survey of channel and radio propagation models for wireless MIMO systems. *EURASIP Journal on Wireless Communications and Networking*, Article ID 19070, Vol. 2007, pp. 1-19.

ASTM E2213–03. (2003). Standard Specification for Telecommunications and Information Exchange Between Roadside and Vehicle Systems — 5 GHz Band Dedicated Short Range Communications (DSRC) Medium Access Control (MAC) and Physical Layer (PHY) Specifications, American Society for Testing Materials (ASTM), West Conshohocken, PA, USA.

Aulin, T. (1979). A modified model for the fading signal at a mobile radio channel. *IEEE Transactions on Vehicular Technology*, Vol. VT-28, No. 3, pp. 182-203.

Bello, P. A. (1963). Characterization of randomly time-variant linear channels. *IEEE Transactions on Communications Systems*, Vol. CM-11, No. 4, pp. 360-393.

Bernadó, L.; Zemen, T.; Paier, A.; Matz, G.; Karedal, J.; Cnik, N.; Dumard, C.; Tufvesson, F.; Hagenauer, M. ; Molisch, A.F. & Mecklenbräuker C. (2008). Non-WSSUS vehicular channel characterization at 5.2 GHz – spectral divergence and time-variant coherence parameters. *XXIX General Assembly of the International Union of Radio Science (URSI)*, Chicago, IL, Aug. 2008.

CEPT Report 101. (2007). *Compatibility Studies in the Band 5855– 5925 MHz between Intelligent Transport Systems (ITS) and other Systems*, European Union Electronic Communications Committee (ECC), within the Conférence Européenne des administrations des Postes et des Télécommunications (CEPT), Bern, Switzeland.

CEPT Report 20. (2007). *The Harmonised Radio Spectrum Use for Safety Critical Applications of Intelligent Transport Systems (ITS)*, European Union Electronic Communications Committee (ECC), within the Conférence Européenne des administrations des Postes et des Télécommunications (CEPT), Bern, Switzeland.

Chen, G. Y.; Huang, S. Y.; Sun, J. S. & Chen, S. Y. (2005). The multi-band dipole antenna. *2005 International Symposium on Communications, Kaohsiung*, Taiwan, Nov. 2005.

Cheng, L.; Henty, B. E.; Stancil, D. D.; Bai, F. & Mudalige. P. (2007). Mobile vehicle-to-vehicle narrowband channel measurement and characterization of the 5.9 GHz dedicated short range communication (DSRC) frequency band. *IEEE Journal on Selected Areas in Communications*, Vol. 25, No. 8, pp. 1501-1526.

Cheng, L.; Henty, B.; Cooper, R.; Stancil, D. D. & Bai, F. (2008a). Multi-path propagation measurements for vehicular networks at 5.9 GHz. *IEEE Wireless Communications and Networking Conference*, pp. 1239-1244, Las Vegas, NV, Ap. 2008.

Cheng, L.; Henty, B. E.; Stancil, D. D.; Bai, F. & Mudalige, P. (2008b). Highway and rural propagation channel modeling for vehicle-to-vehicle communications at 5.9 GHz. *IEEE Antennas and Propagation Society International Symposium*, San Diego, CA, Jul. 2008.

Cheng, L.; Henty, B. E.; Bai, F. & Stancil, D. D. (2008c). Doppler spread and coherence time of rural and highway vehicle-to-vehicle channels at 5.9 GHz. *IEEE Global Telecommunications Conference*, New Orleans, LO, Dec. 2008.

Cheng, X.; Wang, C. X.; Laurenson, D. I.; Salous, S. & Vasilakos, A. V. (2009). An adaptive geometry-based stochastic model for non-isotropic MIMO mobile-to-mobile channels. *IEEE Transactions on Wireless Communications*, Vol. 8, No. 9, pp. 4824-4835.

Clark; R. H. (1968). A statistical theory of mobile radio reception. *Bell Syst. Tech. J.*, Vol. 47, pp. 957-1000.

Emmelmann, M; Bochow B, & Kellum C. (2010). *Vehicular Networking. Automotive Applications and Beyond*, p. 52, Communications Systems for Car-2-X Networks, Wiley.

ETSI EN 300 674. (1999). *Technical Characteristics and Test Methods for Dedicated Short Range Communication (DSRC) Transmission Equipment (500 kbit/s / 250 kbit/s) Operating in the 5.8 GHz Industrial, Scientific and Medical (ISM) Band*, European Telecommunications Standard Institute (ETSI) , Technical Report, Sophia Antipolis, France.

ETSI TR 102 492-1 Part 1. (2006). *Technical Characteristics for Pan European Harmonized Communications Equipment Operating in the 5 Ghz Frequency Range and Intended for Critical Road Safety Applications*, European Telecommunications Standard Institute (ETSI), Technical Report, Sophia Antipolis, France.

ETSI TR 102 492-2 Part 2. (2006). *Technical Characteristics for Pan European Harmonized Communications Equipment Operating in the 5 Ghz Frequency Range Intended for Road Safety and Traffic Management, and for Non-Safety Related ITS Applications*, European Telecommunications Standard Institute (ETSI) , Technical Report, Sophia Antipolis, France.

Gallagher, B. & Akatsuka, H. (2006). Wireless communications for vehicle safety: radio link performance and wireless connectivity methods. *IEEE Vehicular Technonolgy Magazine*, Vol. 1, No. 4, pp. 4-16, 24.

Gradsthteyn, I. S. & Ryzhik I. M. (2007). *Table of Integrals, Series and Products*. San Diego, CA, Academic, 7th ed.

Green, E. & Hata, M. (1991). Microcellular propagation measurements in an urban environment. *IEEE Personal, Indoor and Mobile Radio Communications International Symposium*, pp. 324-328, London, UK, Sep. 1991.

IEEE 802.11. (2007). *Wireless LAN Medium Access Control (MAC) and Physical Layer (PHY) Specifications*, Institute of Electrical and Electronic Engineers (IEEE), New York, USA.

IEEE 802.11p. (2010). Wireless LAN Medium Access Control (MAC) and Physical Layer (PHY) Specifications Amendment 6: Wireless Access in Vehicular Environments, Institute of Electrical and Electronic Engineers (IEEE), New York, USA.

Ito, Y.; Taga, T.; Muramatsu, J. & Susuki, N. (2007). Prediction of line-of-sight propagation loss in inter-vehicle communication environments. *IEEE International Symposium on Personal, Indoor and Mobile Radio Communications*, Athens, Sep. 2007.

Jakes, C. W. (1974). *Microwave Mobile Communications.* Wiley, New York.

Jensen, I. & Halpe Gamage, J. K. (2007). CVIS vehicle rooftop antenna unit, *6th ITS in Europe Congress & Exhibition*, Aalborg, Denmark, Jun. 2007.

Jiang, T.; Chen, H.; Wu, H. & Yi, Y. (2010). Channel modeling and inter-carrier interference analysis for V2V communication systems in frequency-dispersive channels. *Mobile Networks and Applications*, Vol. 15, No. 1, pp. 4-12.

Karedal, J.; Tufvesson, F.; Czink, N.; Paier, A.; Dumard, C.; Zemen, T.; Mecklenbräuker, C. F. & Molisch, A. F. (2009). A geometry-based stochastic MIMO model for vehicle-to-vehicle communications. *IEEE Transactions on Wireless Communications*, Vol. 8, No. 7, pp. 3646-3657.

Kaul, S.; Ramachandran, K.; Shankar, P.; Oh, S.; Gruteser, M.; Seskar, I. & Nadeem, T. (2007). Effect of antenna placement and diversity on vehicular network communications. *IEEE Sensor, Mesh and Ad Hoc Communications and Networks Conference,* pp. 112-121, San Diego, CA, Jun. 2007.

Kim. Y; Song, C.; Koo, I; Choi, H. & Lee S. (2003). Design of a double-looped monopole array antenna for a DSRC system roadside base station. *Microwave and Optical Technology Letters*, Wiley, Vol. 37, No. 1, pp. 74-77.

Kunisch, J. & Pamp, J. (2008). Wideband car-to-car radio channel measurements and model at 5.9 GHz. *IEEE Vehicular Technology Conference*, pp. 1-5, Calgary, BC, Sep. 2008.

Matolak, D. W. (2008). Channel modeling for vehicle-to-vehicle communications. *IEEE Communications Magazine*, Vol. 46 , No. 5, pp. 76-83.

Matolak, D. W. & Wu, K. (2009). Vehicle-to-vehicle channels: Are we done yet?. *IEEE GLOBECOM*, pp. 1-6, Honolulu, HI, Dec. 2009.

Maurer, J.; Fügen, T. & Wiesbeck, W. (2001). A realistic description of the environment for inter-vehicle wave propagation modelling. *IEEE Vehicular Technology Conference*, Vol. 3, pp. 1437-1441, Atlantic City, NJ, Oct. 2001.

Maurer, J.; Fügen, T. & Wiesbeck, W. (2002). Narrow-band measurement and analysis of the inter-vehicle transmission channel at 5.2 GHz. *IEEE Vehicular Technology Conference*, Vol. 3, pp. 1274-1278, Birmingham, AL, May 2002.

Maurer, J.; Fügen, T.; Schäfer, T. & Wiesbeck, W. (2004). A new inter-vehicle communications (IVC) channel model. *IEEE Vehicular Technology Conference*, Vol. 1, pp. 9-13, Los Angeles, CA, Sep. 2004.

Michelson, D. G. & Ghassemzadeh, S. S. (2009). *New Directions in Wireless Communications Research*. Springer Science+Business Media (Chapter 1).

Molisch, A. F. & Tufvesson, F. (2004). Multipath propagation models for broadband wireless systems. *CRC Handbook of signal processing for wireless communications*, Chapter 2, 2004.

Molisch, A. F. (2005). *Wireless Communications*, IEEE Press-Wiley.

Molisch, A. F.; Tufvesson, F.; Karedal, J. & Mecklenbräuker, C. (2009). A survey on vehicle-to-vehicle propagation channels. *IEEE Wireless Communications*, Vol. 16, No. 6, pp. 12-22.

Paier, A.; Karedak, J; Czink, N.; Hofstetter, H.; Dumand, C.; Zemen, T.; Tufvesson, F.; Mecklenbräuker, C. F. & Molisch, A. F. (2007). First results from car-to-car and car-to-car infrastructure radio channel measurements at 5.2 GHz. *IEEE International Symposium on Personal, Indoor and Mobile Radio Communications*, Athens, Sep. 2007.

Parsons, J. D. (2000). *The Mobile Radio Propagation Channel*, 2nd ed., Wiley, New York.

Paschalidis, P.; Wisotzki, M.; Kortke, A.; Keusgen, W. & Peter, M. (2008). A wideband channel sounder for car-to-car radio channel measurements at 5.7 GHz and results for an urban scenario. *IEEE Vehicular Technology Conference*, Calgary, BC, Sep. 2008.

Peden, M.; Scurfield, R.; Sleet, D. ; Mohan, D. ; Hyder, A. A. ; Jarawan, E. & Mathers, C. (2004). *World Report on Road Traffic Injury Prevention*, pp. 31-66, World Health Organization, Geneva, Switzerland.

Renaudin, O.; Kolmonen, V-M.; Vainikainen, P. & Oestges, C. (2009). Car-to-car channel models based on wideband MIMO measurements at 5.3 GHz. *European Conference on Antennas and Propagation*, pp. 635-639, Berlin, Germany, Mar. 2009.

Renaudin, O.; Kolmonen, V-M.; Vainikainen, P. & Oestges, C. (2010). Non-stationary narrowband MIMO inter-vehicle channel characterization in the 5-GHz band. *IEEE Transactions on Vehicular Technology*, Vol. 59, No. 4, pp. 2007-2015.

Sai, S.; Niwa, E.; Mase, K.; Nishibori, M.; Inoue J.; Obuchi, M.; Harada, T.; Ito, H.; Mizutani, K. & Kizu, M. (2009). Field evaluation of UHF radio propagation for an ITS safety system in an urban environment, *IEEE Communications Magazine*, Vol. 47, No. 11, pp. 120-127, Nov. 2009.

Sen, I. & Matolak, D. W. (2007). V2V channels and performance of multiuser spread spectrum modulation. *IEEE Vehicular Technology Magazine*, Vo. 2, No. 4, pp. 19-25.

Sen, I. & Matolak, D. W. (2008). Vehicle-vehicle channel models for the 5-GHz band. *IEEE Transactions on Intelligent Transportation Systems*, Vol. 9, No. 2, pp. 235-245.

Sklar, B. (1997). Rayleigh fading channels in mobile digital communication systems part i: characterization. *IEEE Communications Magazine*, Vol. 35, No. 7, pp. 90-100.

Tan, I.; Tang, W.; Laberteaux, K. & Bahai, A. (2008) Measurement and analysis of wireless channel impairments in DSRC vehicular communications. *IEEE International Conference on Communications*, pp. 4882-4888, Beijing, China, May 2008.

Vlacic, L; Parent, M. & Harashima, F. (2001). *Intelligent Vehicle Technologies. Theory and Applications*, pp. 87-188, Butterworth-Heinemann, Oxford, UK.

Wan, R. & Cox, D. (2002). Channel modeling for ad hoc mobile wireless networks. *IEEE Vehicular Technology Conference*, Vol. 1, pp. 21-25, Birmingham, AL, May 2002.

Wan, L. C. & Cheng, Y. H. Cheng. (2005). A statistical mobile-to-mobile Rician fading channel model. *IEEE Vehicular Technology Conference*, Vol. 1, pp. 63-67, Stockholm, Sweden, May 2005.

Wang, C. X.; Cheng X. & Laurenson D. I. (2009). Vehicle-to-vehicle channel modeling and measurements: recent advances and future challenges. *IEEE Communications Magazine*, Vol. 47, No. 11, pp. 96-103.

Wu, Q.; Matolak, D. W. & Sen. I. (2010). 5-GHz-band vehicle-to-vehicle channels: models for multiple values of channel bandwidth. *IEEE Transactions on Vehicular Technology*, Vol. 59, No. 5, pp. 2620-2625.

Xia, H. H.; Bertoni, H. L.; Maciel, L. R.; Lindsay-Stewart, A. & Rowe, R. (1993). Radio propagation characteristics for line-of-sight microcellular and personal communications. *IEEE Transactions on Antennas and Propagation*, Vol. 41, No. 10, pp. 1439-1447.

WINNER European Project. (2007), D1.1.2. WINNER II Channel models. Part II Channel measurement and analysis results.
[Online] Available: http://www.ist-winner.org/deliverables.html

Zajic, A. & Stüber, G. L. (2008). Space-time correlated mobile-to-mobile channels: modelling and simulation. *IEEE Transactions on Vehicular Technology*, Vol. 57, No. 2, pp. 715-726.

Zajic, A. & Stüber, G. L. (2009). Wideband MIMO mobile-to-mobile channels: geometry-based statistical modeling with experimental verification. *IEEE Transactions on Vehicular Technology*, Vol. 58, No. 2, pp. 517-534.

Zheng, Y.R. (2006). A non-isotropic model for mobile-to-mobile fading channel simulations. *IEEE Military Communications Conference*, Washington, Oct. 2006.

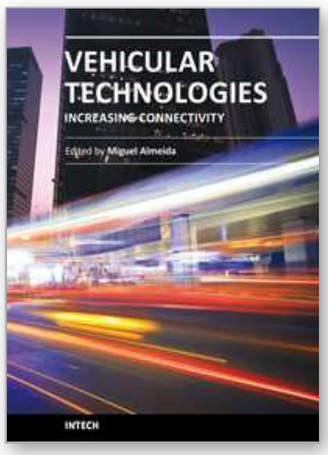

Vehicular Technologies: Increasing Connectivity
Edited by Dr Miguel Almeida

ISBN 978-953-307-223-4
Hard cover, 448 pages
Publisher InTech
Published online 11, April, 2011
Published in print edition April, 2011

This book provides an insight on both the challenges and the technological solutions of several approaches, which allow connecting vehicles between each other and with the network. It underlines the trends on networking capabilities and their issues, further focusing on the MAC and Physical layer challenges. Ranging from the advances on radio access technologies to intelligent mechanisms deployed to enhance cooperative communications, cognitive radio and multiple antenna systems have been given particular highlight.

How to reference
In order to correctly reference this scholarly work, feel free to copy and paste the following:

Lorenzo Rubio, Juan Reig and Herman Fernández (2011). Propagation Aspects in Vehicular Networks, Vehicular Technologies: Increasing Connectivity, Dr Miguel Almeida (Ed.), ISBN: 978-953-307-223-4, InTech, Available from: http://www.intechopen.com/books/vehicular-technologies-increasing-connectivity/propagation-aspects-in-vehicular-networks

INTECH
open science | open minds

InTech Europe
University Campus STeP Ri
Slavka Krautzeka 83/A
51000 Rijeka, Croatia
Phone: +385 (51) 770 447
Fax: +385 (51) 686 166
www.intechopen.com

InTech China
Unit 405, Office Block, Hotel Equatorial Shanghai
No.65, Yan An Road (West), Shanghai, 200040, China
中国上海市延安西路65号上海国际贵都大饭店办公楼405单元
Phone: +86-21-62489820
Fax: +86-21-62489821

IntechOpen